Carbonio, suoi stati allotropici e Grafite

M. Riccò

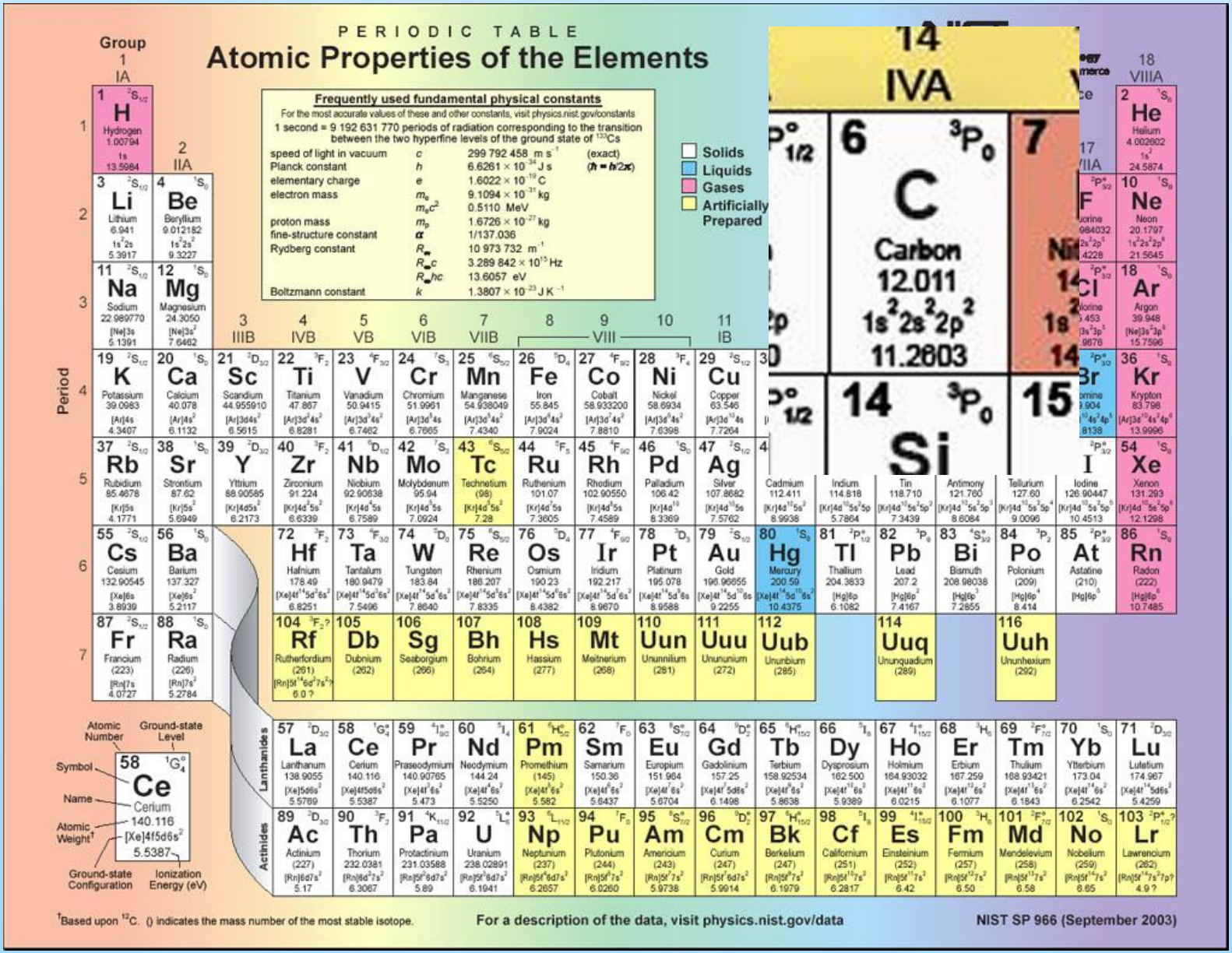
PERIODIC TABLE
Atomic Properties of the Elements
Group
1
IA
2
IIA
3
IIIB
4
IVB
5
VB
6
VIB
7
VIIB
8
9
10
VIII
11
IB
14
IVA
17
VIIA
18
VIIIA
Period
Frequently used fundamental physical constants
For the most accurate values of these and other constants, visit physics.nist.gov/constants
1 second = 9 192 631 770 periods of radiation corresponding to the transition between the two hyperfine levels of the ground state of 133Cs
speed of light in vacuum c 299 792 458 m s-1 (exact)
Planck constant h 6.6261 × 10-34 J s (ħ = h/2π)
elementary charge e 1.6022 × 10-19 C
electron mass me 9.1094 × 10-31 kg
mec2 0.5110 MeV
proton mass mp 1.6726 × 10-27 kg
fine-structure constant α 1/137.036
Rydberg constant R∞ 10 973 732 m-1
R∞c 3.289 842 × 10+15 Hz
R∞hc 13.6057 eV
Boltzmann constant k 1.3807 × 10-23 J K-1
Solids
Liquids
Gases
Artificially Prepared
6 3P0 C Carbon 12.011 1s2 2s2 2p2 11.2803
14 3P0 Si
Lanthanides
Actinides
Atomic Number
Ground-state Level
Symbol
Name
Atomic Weight†
Ground-state Configuration
Ionization Energy (eV)
58 1G4° Ce Cerium 140.116 [Xe]4f5d6s2 5.5387
†Based upon 12C. () indicates the mass number of the most stable isotope.
For a description of the data, visit physics.nist.gov/data
NIST SP 966 (September 2003)

- Isotopo ^{12}C → abbondanza naturale (98.93%, S=0)
- Isotopo ^{13}C → importante per l'NMR (1.07%, S=1/2)
- Isotopo ^{14}C → importante per la datazione archeologica (vita media 5730 anni)

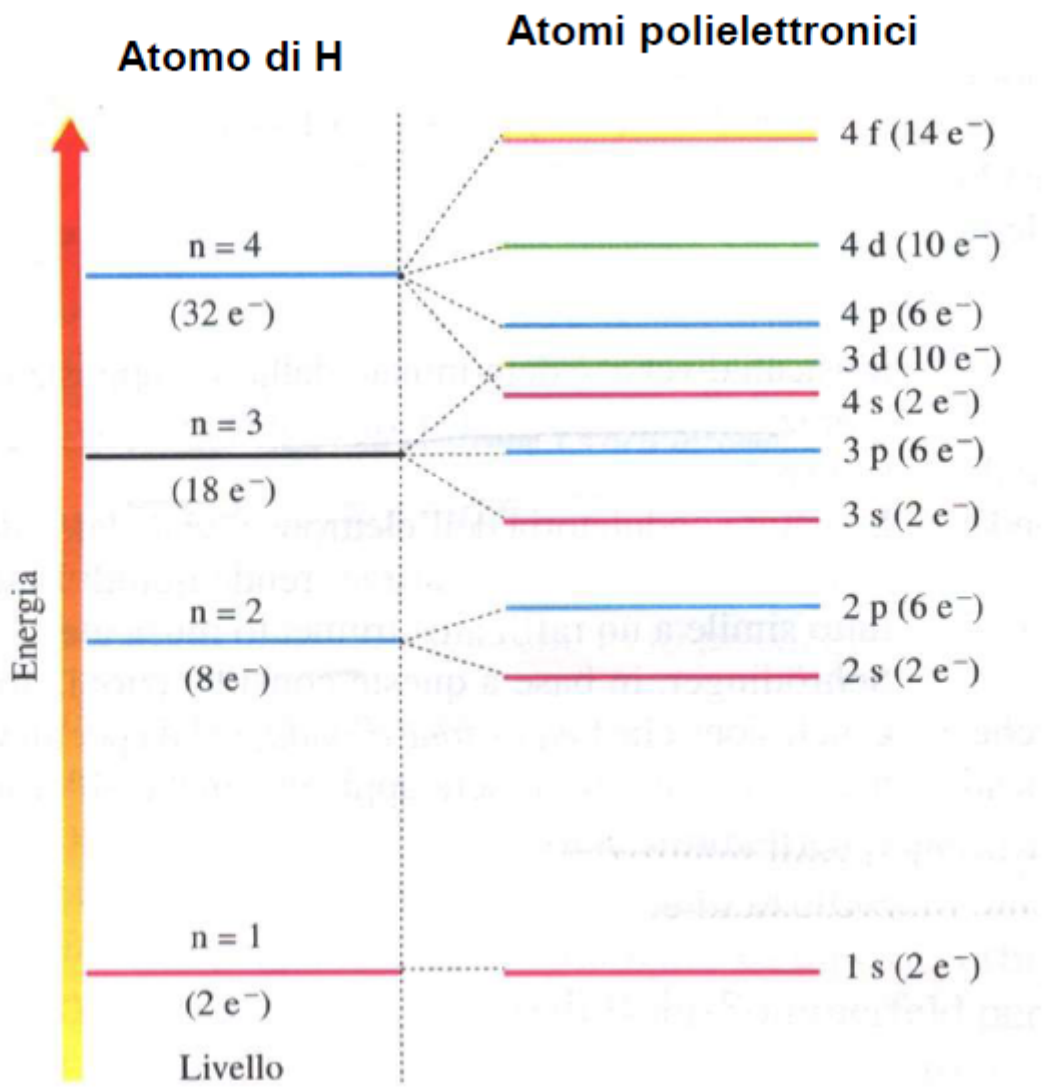

L'energia di ogni elettrone negli atomi polielettronici dipende non solo da n, ma anche da l; conseguenza fondamentale delle interazioni interelettroniche

Scissione dei livelli energetici in più sottolivelli distinti di energia crescente, per un dato valore di n, con il crescere di l.

Tra il livello 3 ed il livello 4 vi è una sovrapposizione dei livelli energetici

Ibridizzazione sp^3

Configurazione: [He] $2s^2$ $2p^2$

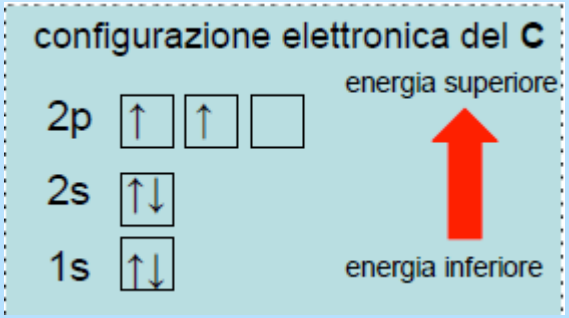

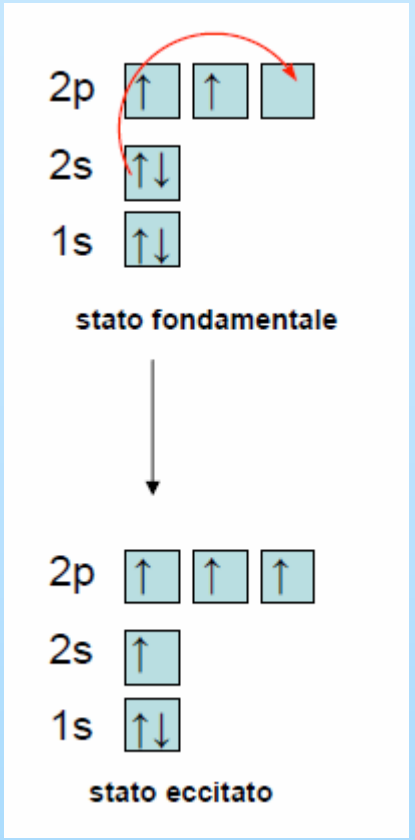

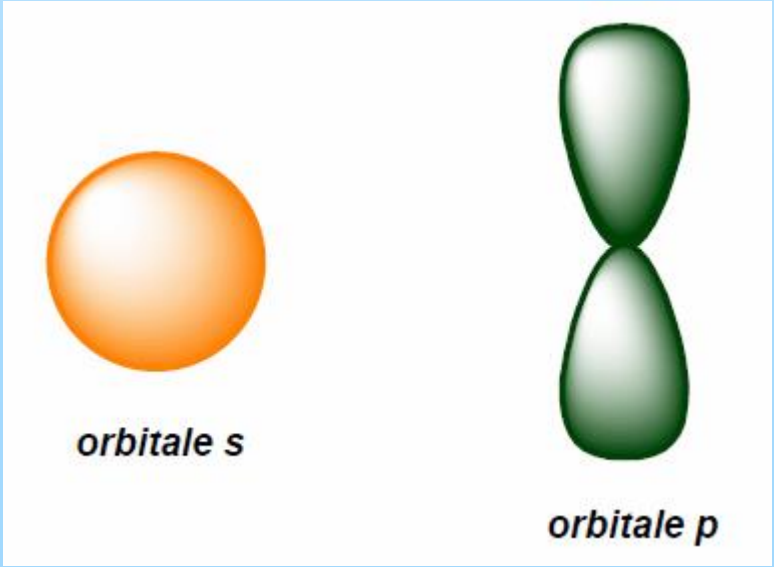

Ibridizzazione sp^3

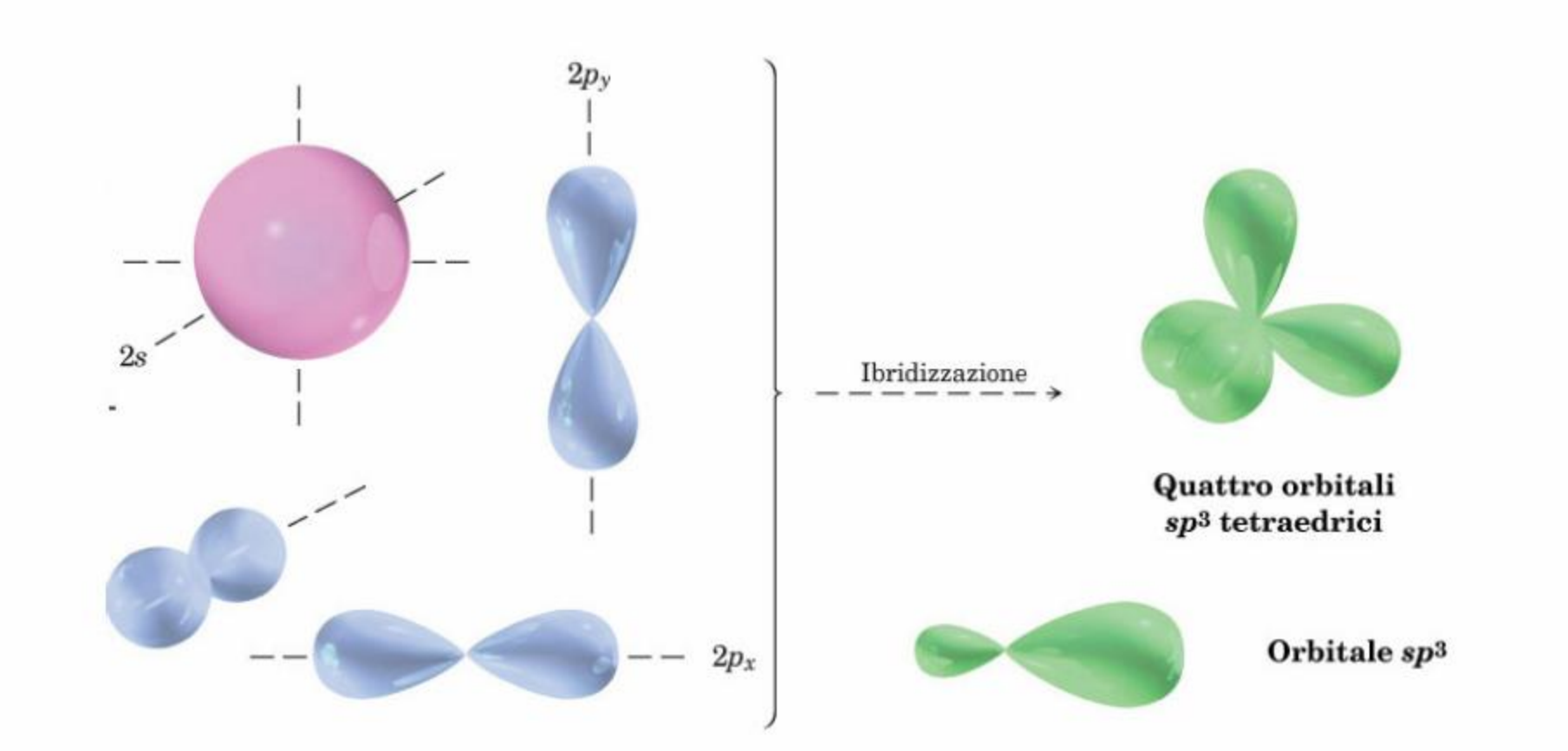

Ibridizzazione sp^3

Metano

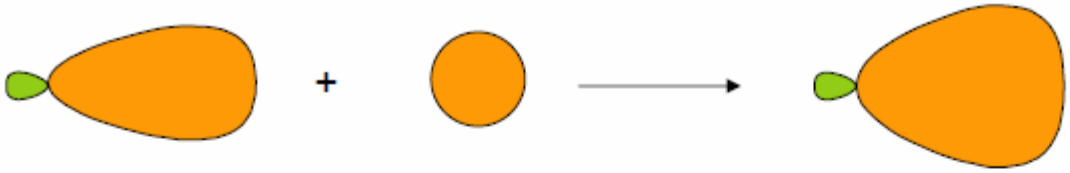

orbitale sp^3 del carbonio

orbitale s dell'idrogeno

orbitale σ C-H

L'angolo di legame formato da ciascun H-C-H vale esattamente 109,5° (angolo tetraedrico)

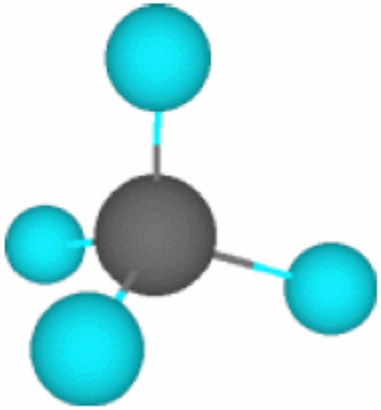

Ibridizzazione sp^2

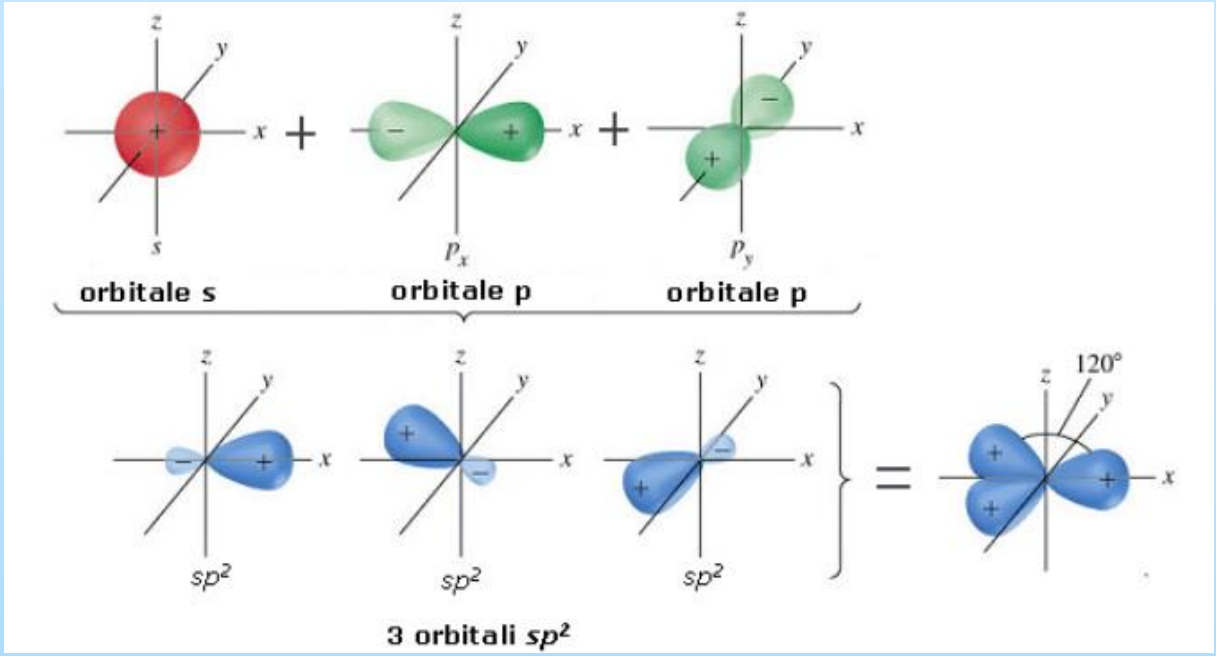

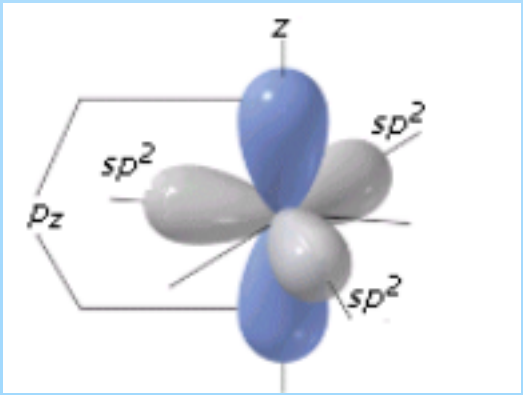

Ibridizzazione sp^2

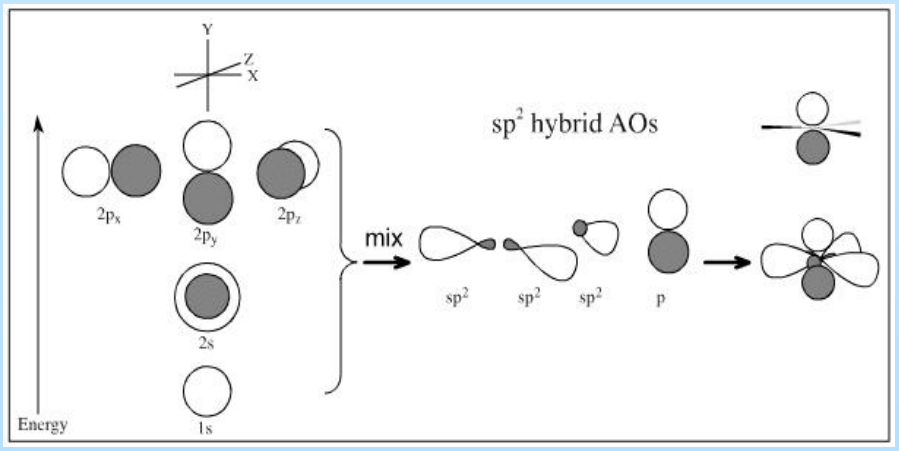

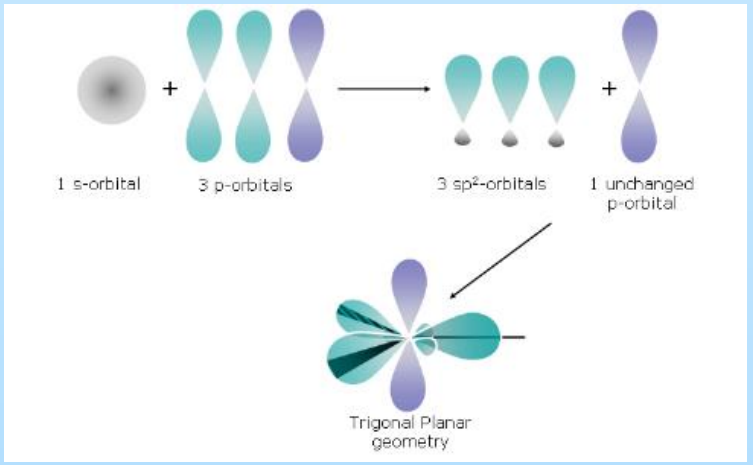

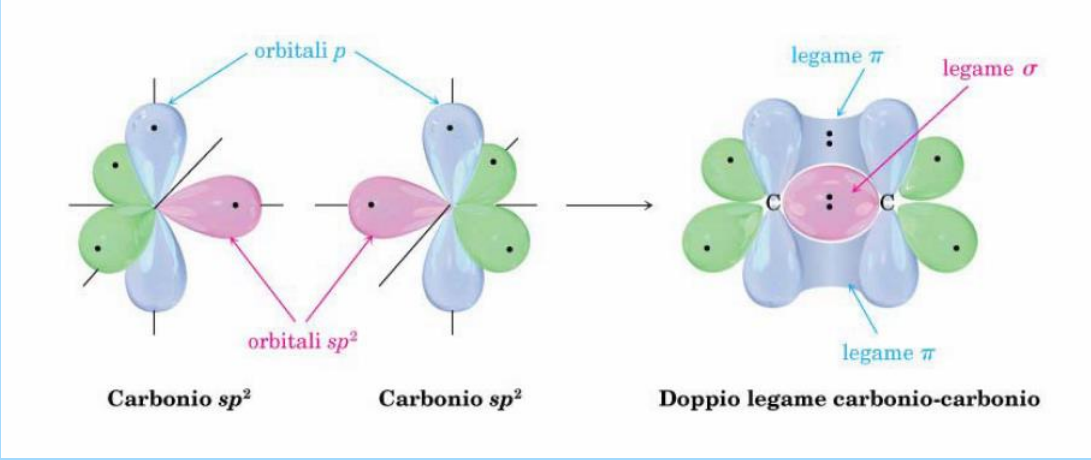

Ibridizzazione sp^2

Etilene

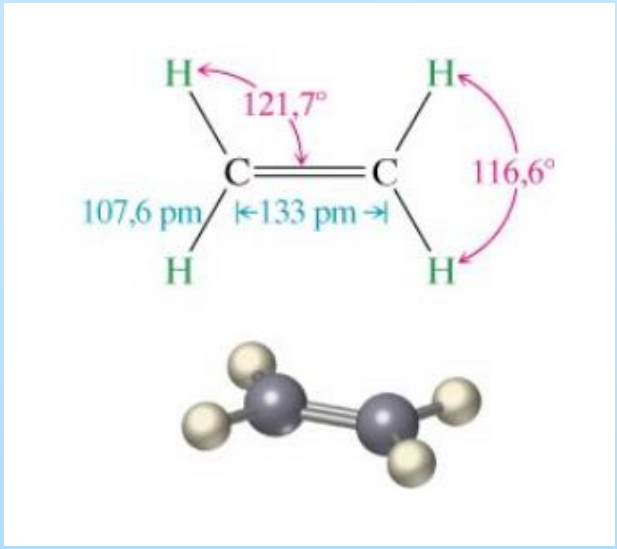

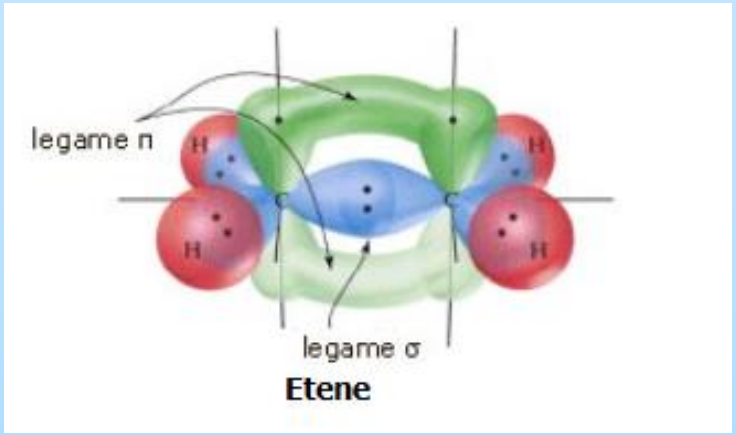

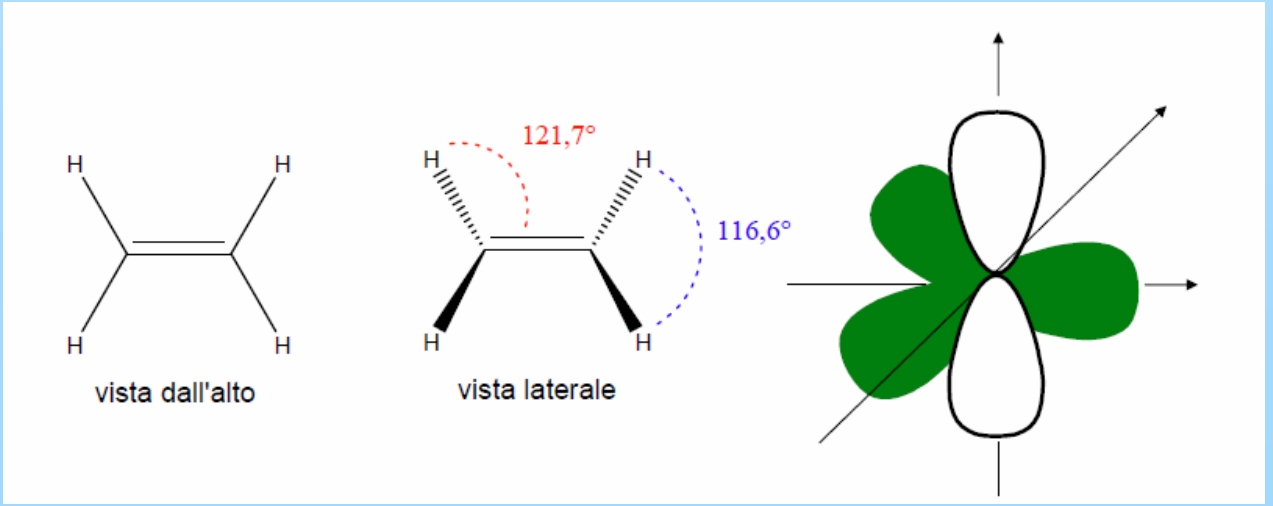

Ibridizzazione sp

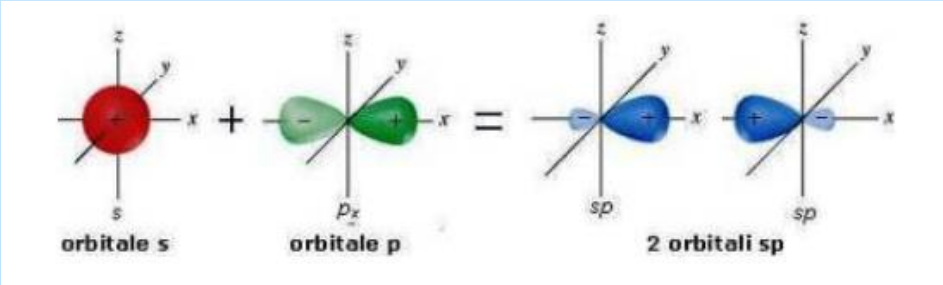

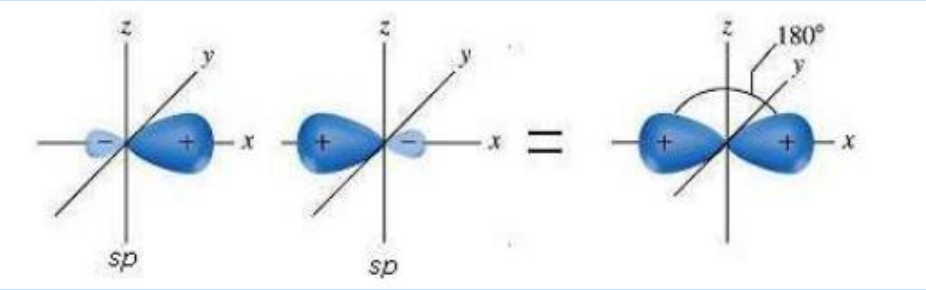

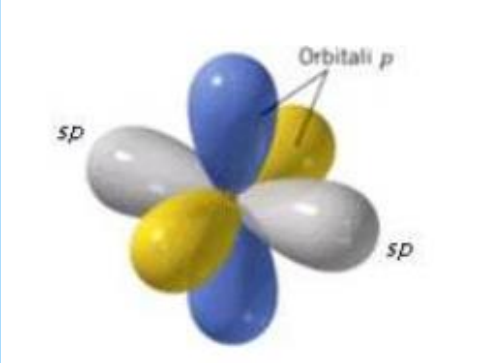

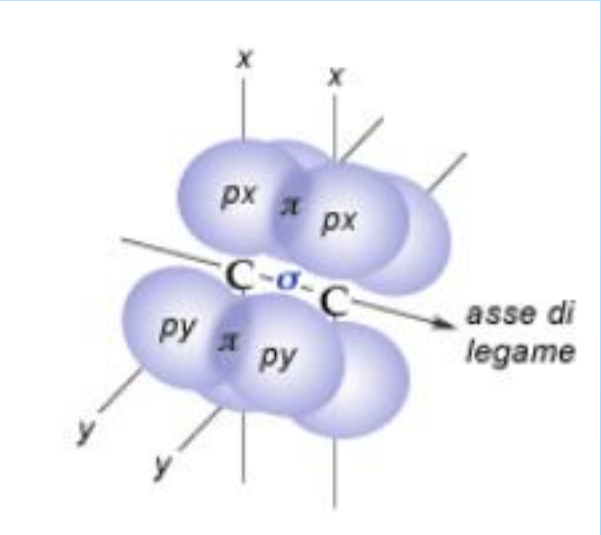

Ibridizzazione sp

Acetilene

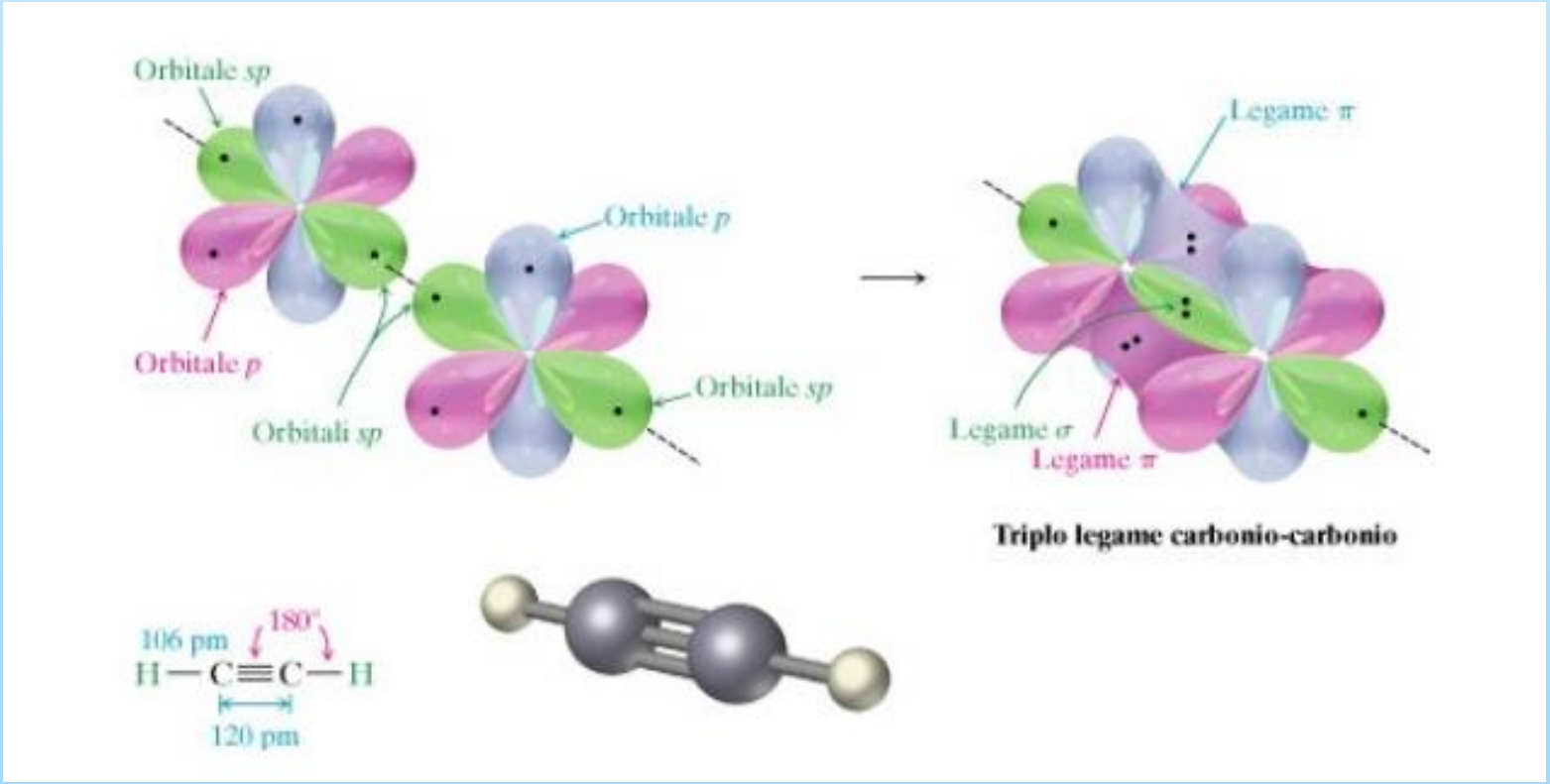

Ibridizzazione sp^n

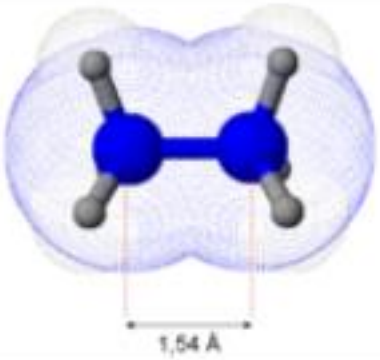	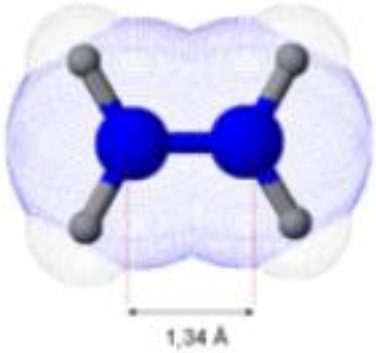	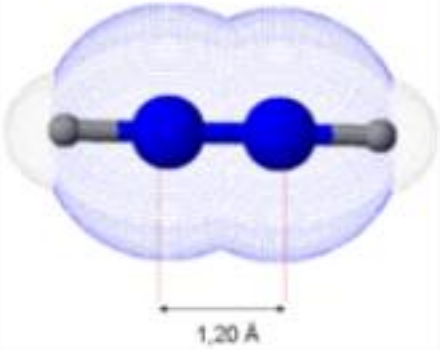
1,54 Å	1,34 Å	1,20 Å
Legame singolo Carbonio-Carbonio	Legame doppio Carbonio-Carbonio	Legame triplo Carbonio-Carbonio
Ibridizzazione sp^3	Ibridizzazione sp^2	Ibridizzazione sp

Stati allotropici del carbonio

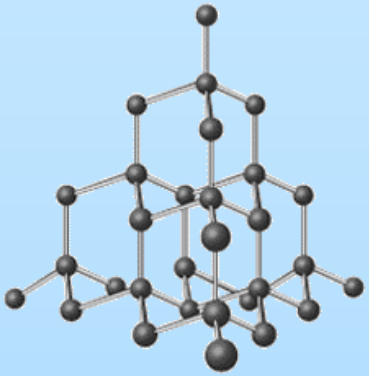

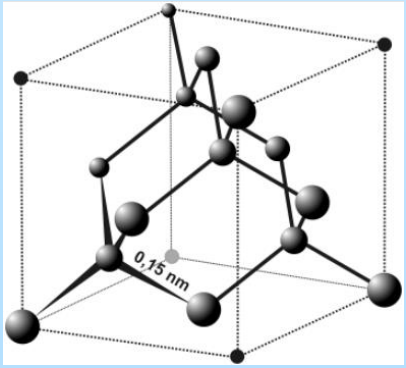

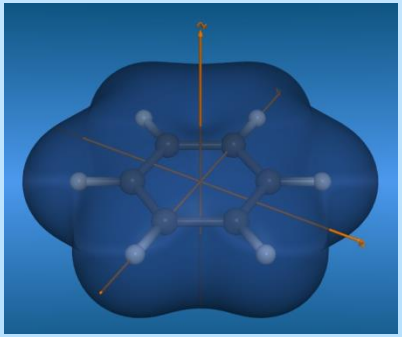

Diamante

Grafite

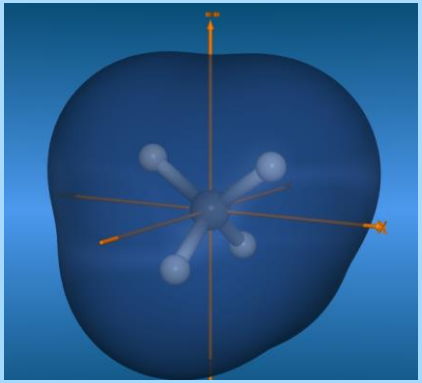

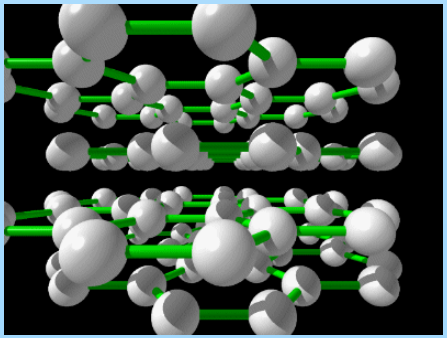

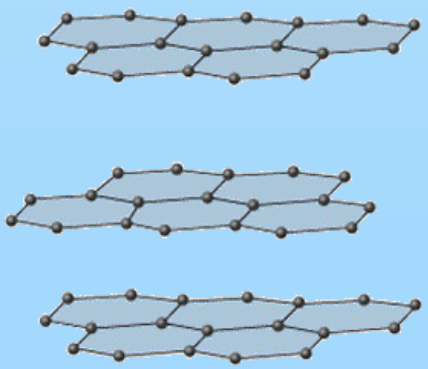

Ibridizzazione *sp*

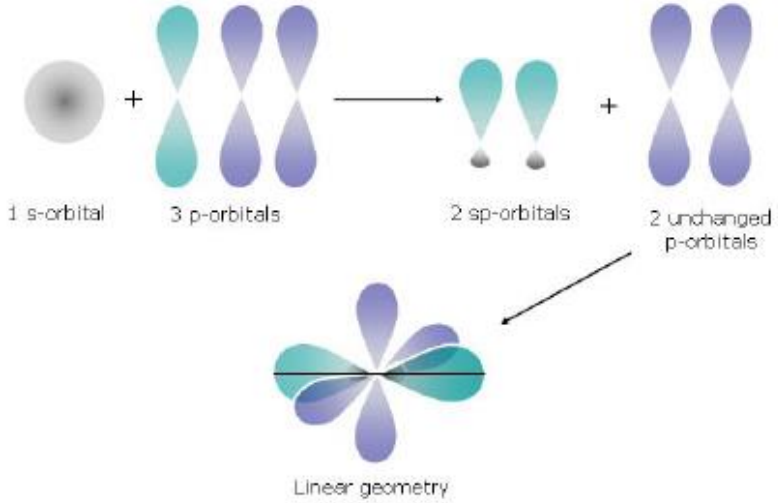

Due possibilità: (a) ***poliini***, alternanza legami tripli e doppi

(b) ***cumuleni***, catena di legami doppi

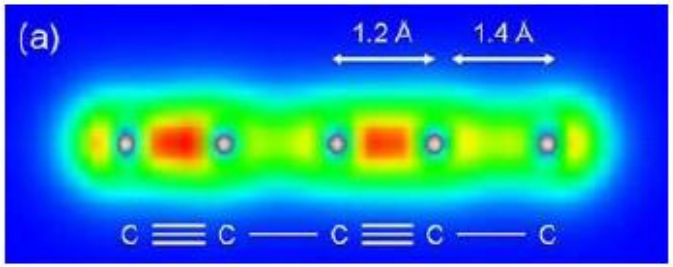

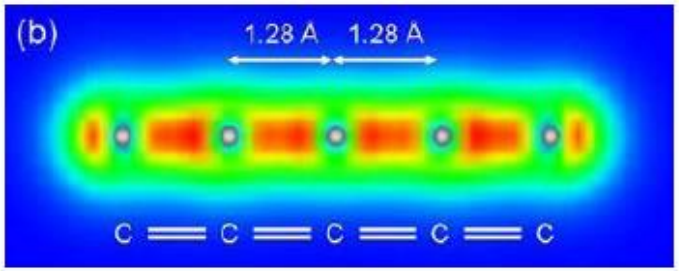

<u>Problema</u>: i sistemi di carbonio *sp* sono instabili

- reattività delle catene insature (es. O_2);
- tendenza a formare *cross-links* fra le catene, favorendo l'evoluzione verso la più stabile fase sp^2.

Catene *sp* isolate sono state osservate solo in fase gassosa o in matrici di gas inerti a basse temperature.

Chaoite

REPORTS

A New Allotropic Form of Carbon from the Ries Crater

A. El Goresy[1], G. Donnay[1]
+ See all authors and affiliations

Science 26 Jul 1968:
Vol. 161, Issue 3839, pp. 363-364
DOI: 10.1126/science.161.3839.363

Abstract

A new allotropic form of carbon occurs in shock-fused graphite gneisses in the Ries Crater, Bavaria. The assemblage in which it occurs consists of hexagonal graphite, rutile, pseudobrookite, magnetite, nickeliferous pyrrhotite, and baddeleyite. Electron-probe analyses indicate that the new phase is pure carbon. It is opaque and much more strongly reflecting than hexagonal graphite. Measurement of x-ray diffraction powder patterns leads to cell dimensions a = 8.948 ± 0.009, c = 14.078 ± 0.017 angstroms, with a primitive hexagonal lattice.

Science
Vol 161, Issue 3839
26 July 1968

Stati allotropici del carbonio

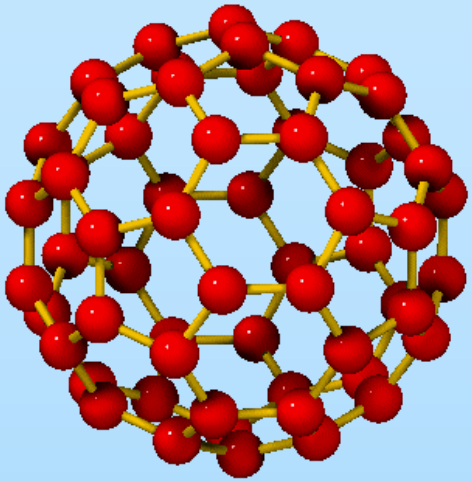

Fullerene (C_{60})

Curl, Kroto e Smalley,
premio Nobel per la Chimica 1996

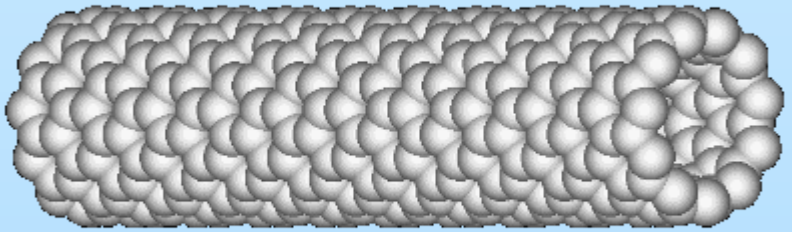

Nanotubi

(Iijima 1991)

Nanostrutture……

GRAPHENE ALLOTROPES

3D

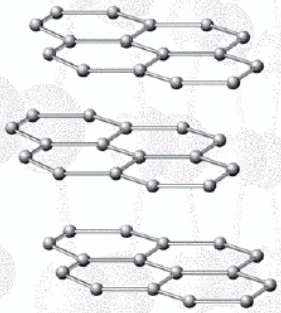

Graphite

2D

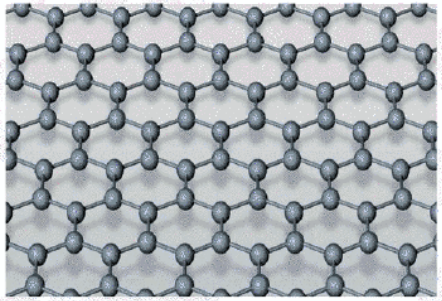

graphene

PRESUMED
NOT TO EXIST
IN THE FREE STATE

1D

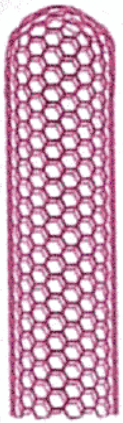

Carbon Nanotube

multi-wall:
1952 to *Iijima 1991*
single-wall: 1993

0D

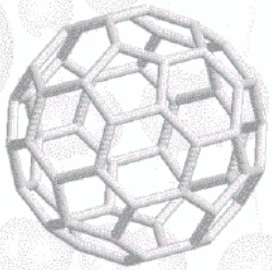

Buckyballs

Kroto et al 1985

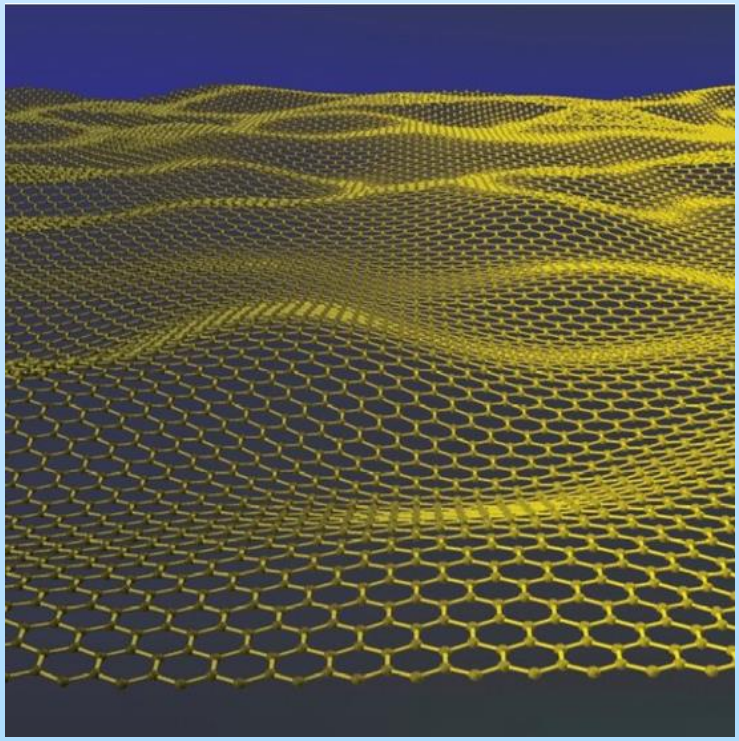

Grafene

K. Novoselov, A. Geim

Premio Nobel per la Fisica 2010

Diamante ↔ Grafite

Table 2.1

Properties of graphite and diamond

Property	Graphite[a]		Diamond
Lattice structure	Hexagonal		Cubic
Space group	$P6_3/mmc$ (D^4_{6h})		$Fd3m$ (O^7_h)
Lattice constant[b] (Å)	2.462	6.708	3.567
Atomic density (C atoms/cm³)	1.14×10^{23}		1.77×10^{23}
Specific gravity (g/cm³)	2.26		3.515
Specific heat (cal/g·K)	0.17		0.12
Thermal conductivity[b] (W/cm·K)[c]	30	0.06	~25
Binding energy (eV/C atom)	7.4		7.2
Debye temperature (K)	2500	950	1860
Bulk modulus (GPa)	286		42.2
Elastic moduli (GPa)	1060[d]	36.5[d]	107.6[e]
Compressibility (cm²/dyn)	2.98×10^{-12}		2.26×10^{-13}
Mohs hardness[f]		9	10
Band gap (eV)	−0.04[g]		5.47
Carrier density (10^{18}/cm³ at 4 K)	5		0
Electron mobility[b] (cm²/Vsec)	20,000	100	1800
Hole mobility[b] (cm²/Vsec)	15,000	90	1500
Resistivity (Ωcm)	50×10^{-6}	1	$\sim10^{20}$
Dielectric constant[b] (low ω)	3.0	5.0	5.58
Breakdown field (V/cm)	0		10^7 (highest)
Magnetic susceptibility (10^{-6}cm³/g)	−0.5	−21	—
Refractive index (visible)			2.4
Melting point (K)	4450		4500
Thermal expansion[b] (/K)	-1×10^{-6}	29×10^{-6}	$\sim1\times10^{-6}$
Velocity of sound (cm/sec)	$\sim2.63\times10^5$	$\sim1\times10^5$	$\sim1.96\times10^5$
Highest Raman mode (cm⁻¹)	1582		1332

[a] For anisotropic properties, the in-plane (ab plane or a-axis) value is given on the left and the c-axis value on the right.

[b] Measurements at room temperature (300 K).

[c] Highest reported thermal conductivity values are listed.

[d] In-plane elastic constant is C_{11} and c-axis value is C_{33}. Other elastic constants for graphite are $C_{12} = 180$, $C_{13} = 15$, $C_{44} = 4.5$ GPa.

[e] For diamond, there are three elastic constants, $C_{11} = 1040$, $C_{12} = 170$, $C_{44} = 550$ GPa.

[f] A scale based on values from 0 to 10, where 10 is the hardest material (diamond) and 1 is talc [2.8].

[g] A negative band gap implies a band overlap, i.e., semimetallic behavior.

Diagramma di Fase

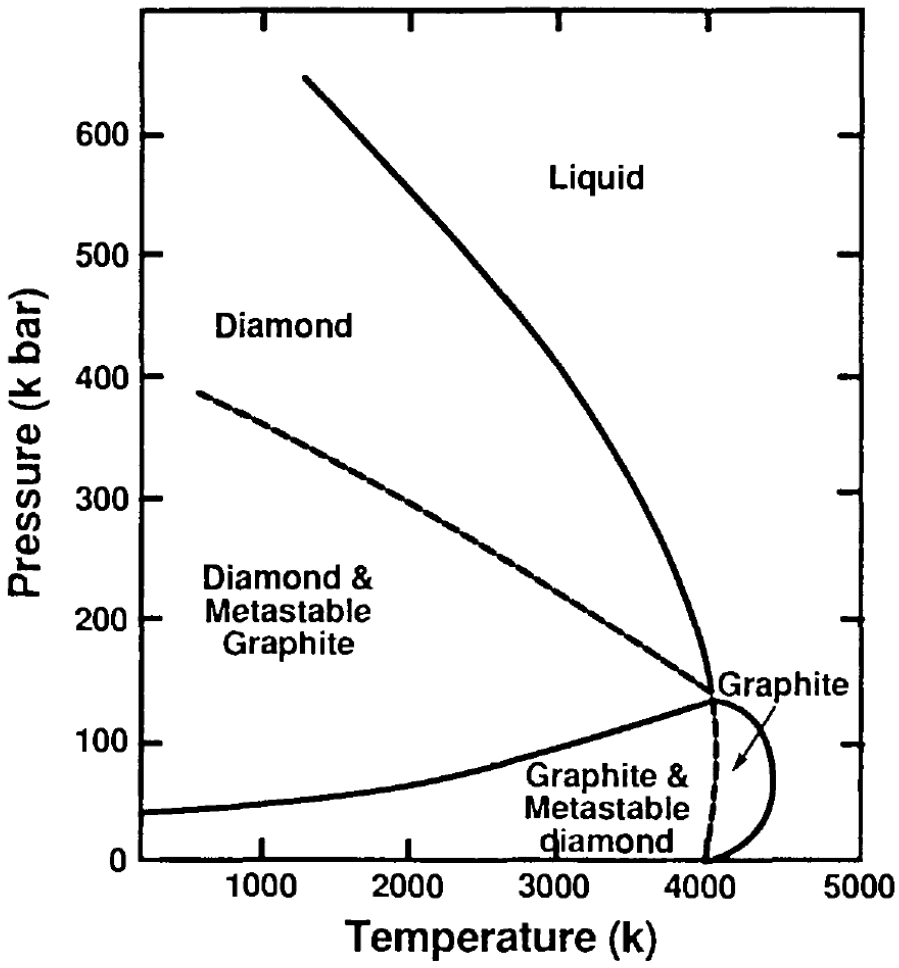

Figure 2.20. Carbon phase diagram.

Sintesi dei diamanti

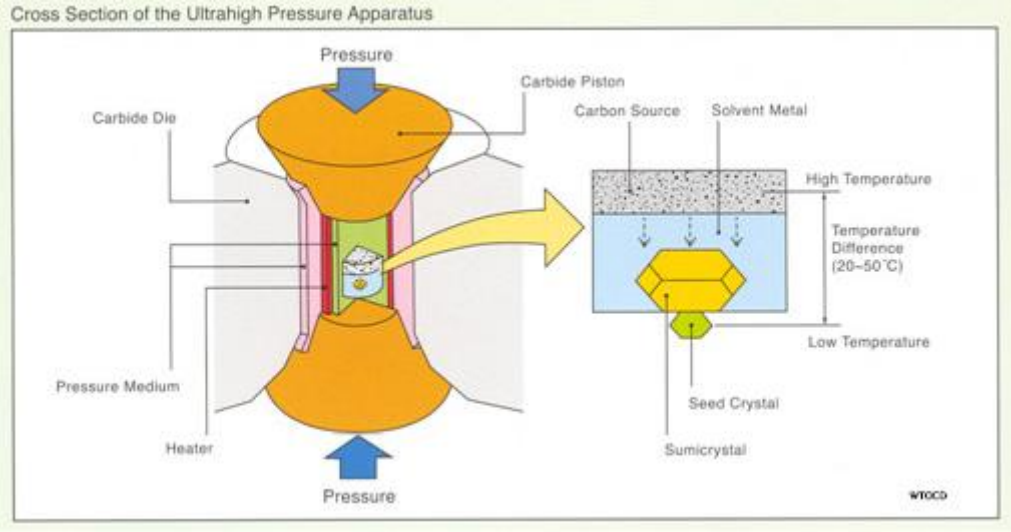


US Synthetic Cubic Press

Ibridizzazione sp^2

Configurazione: [He] $2s^2$ $2p^2$

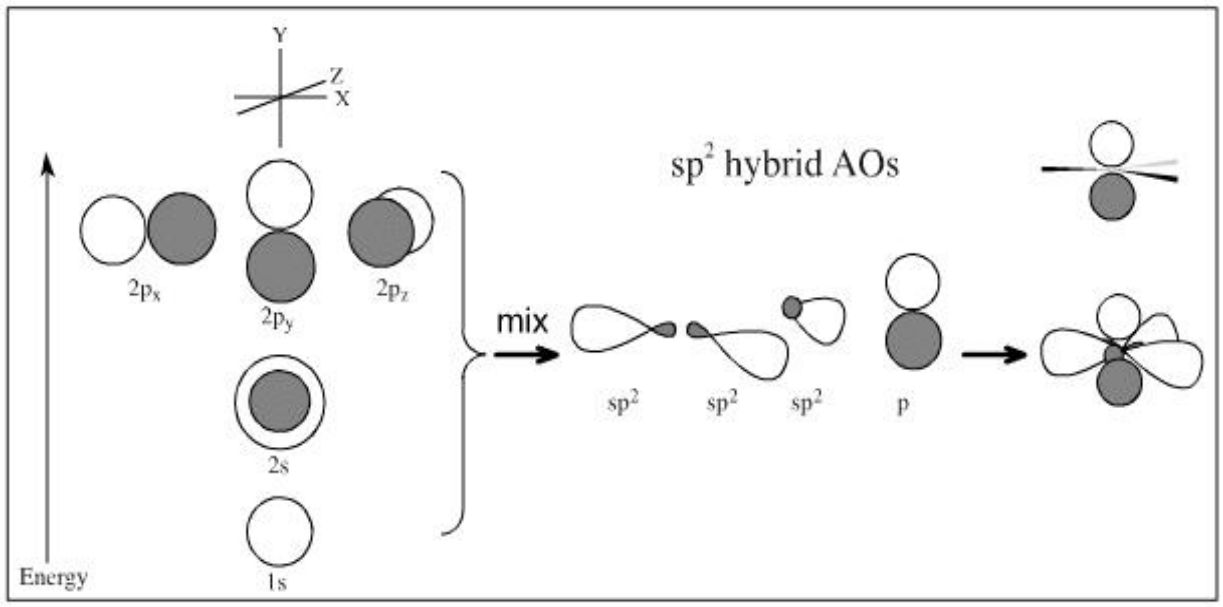

Ibridizzazione sp^2: benzene

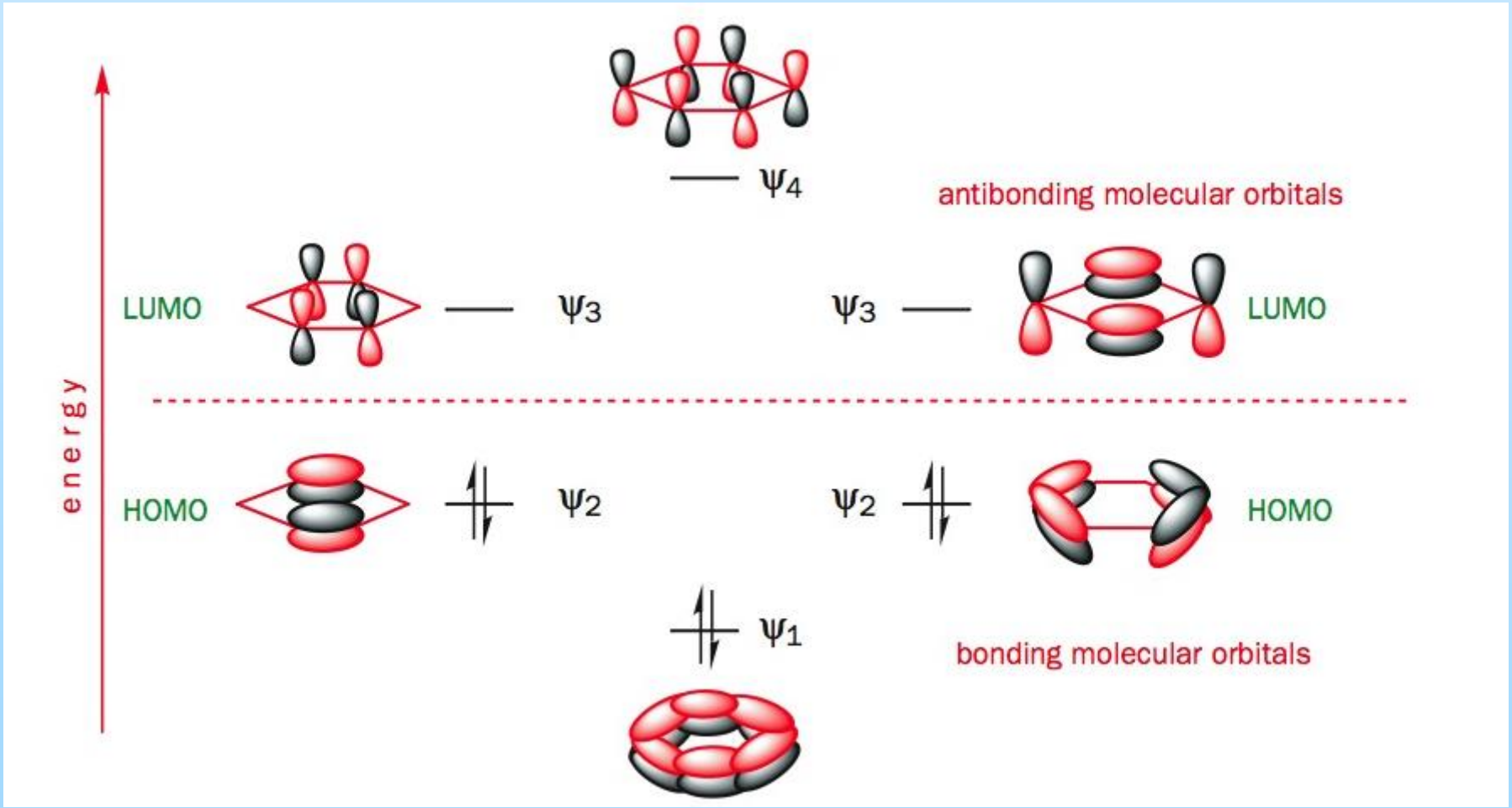

Ibridizzazione sp^2: grafene

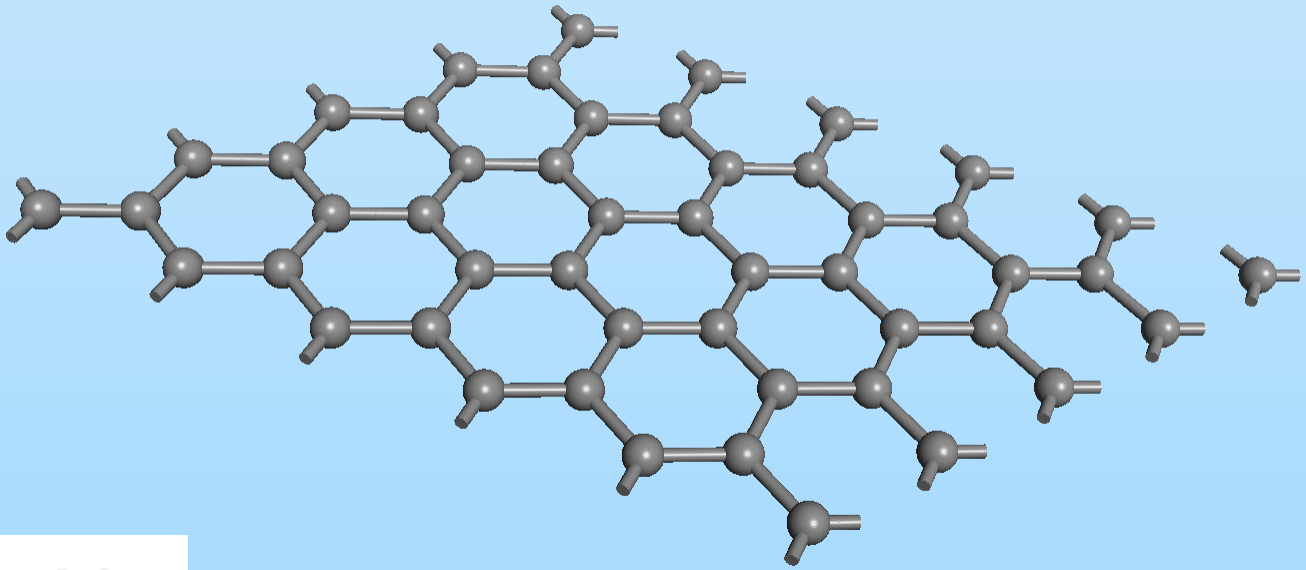

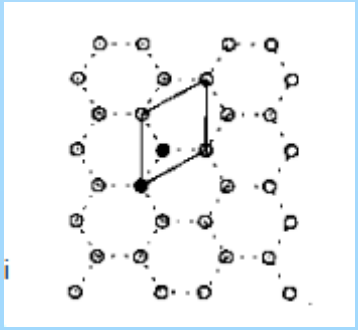

Grafite Struttura

grafite esagonale

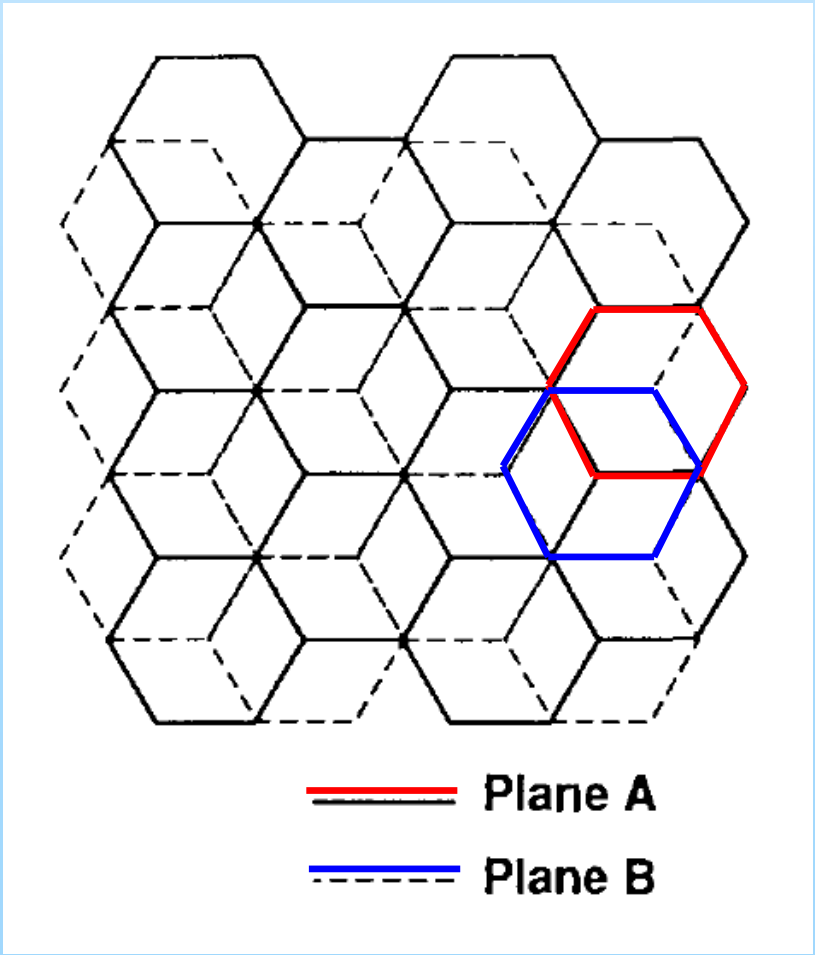

grafite romboedrica

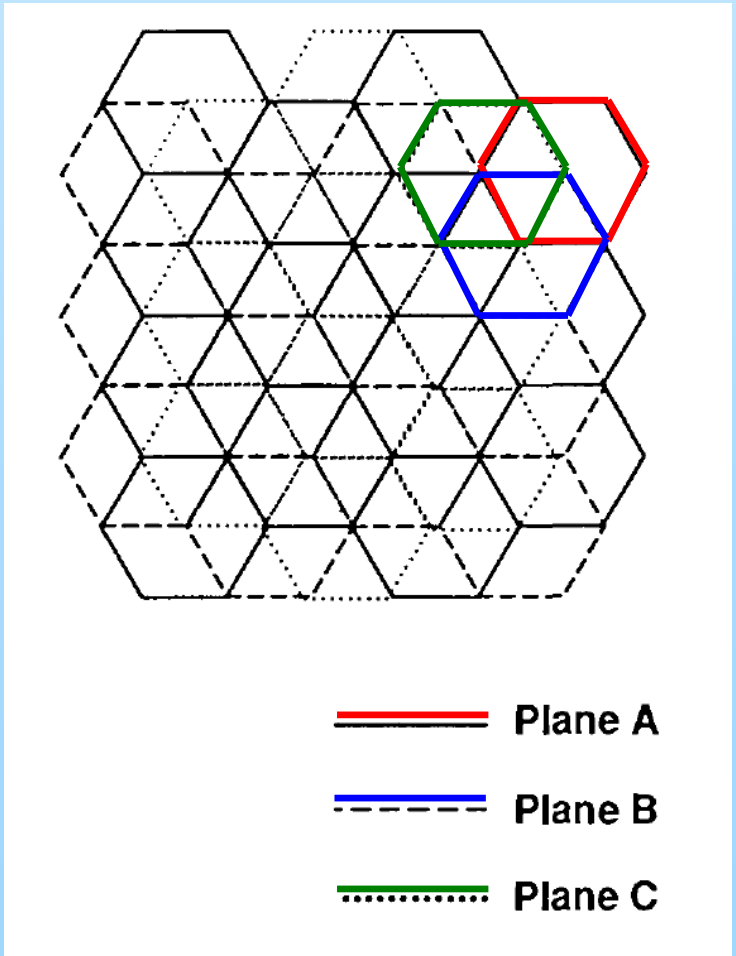

Grafite esagonale: cella unitaria

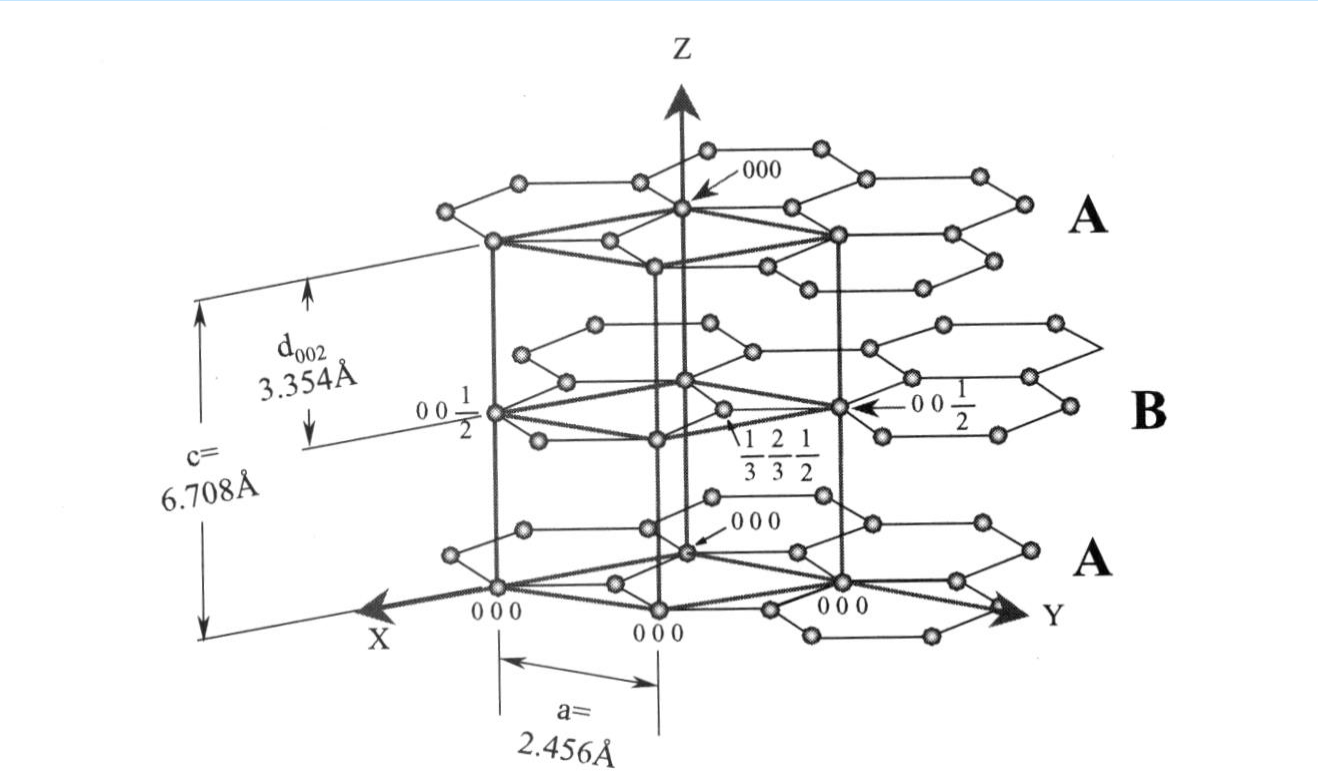

d(C=C) = 1.42 Å

Grafite cella unitaria

Gruppo esagonale P 63 MMC #194

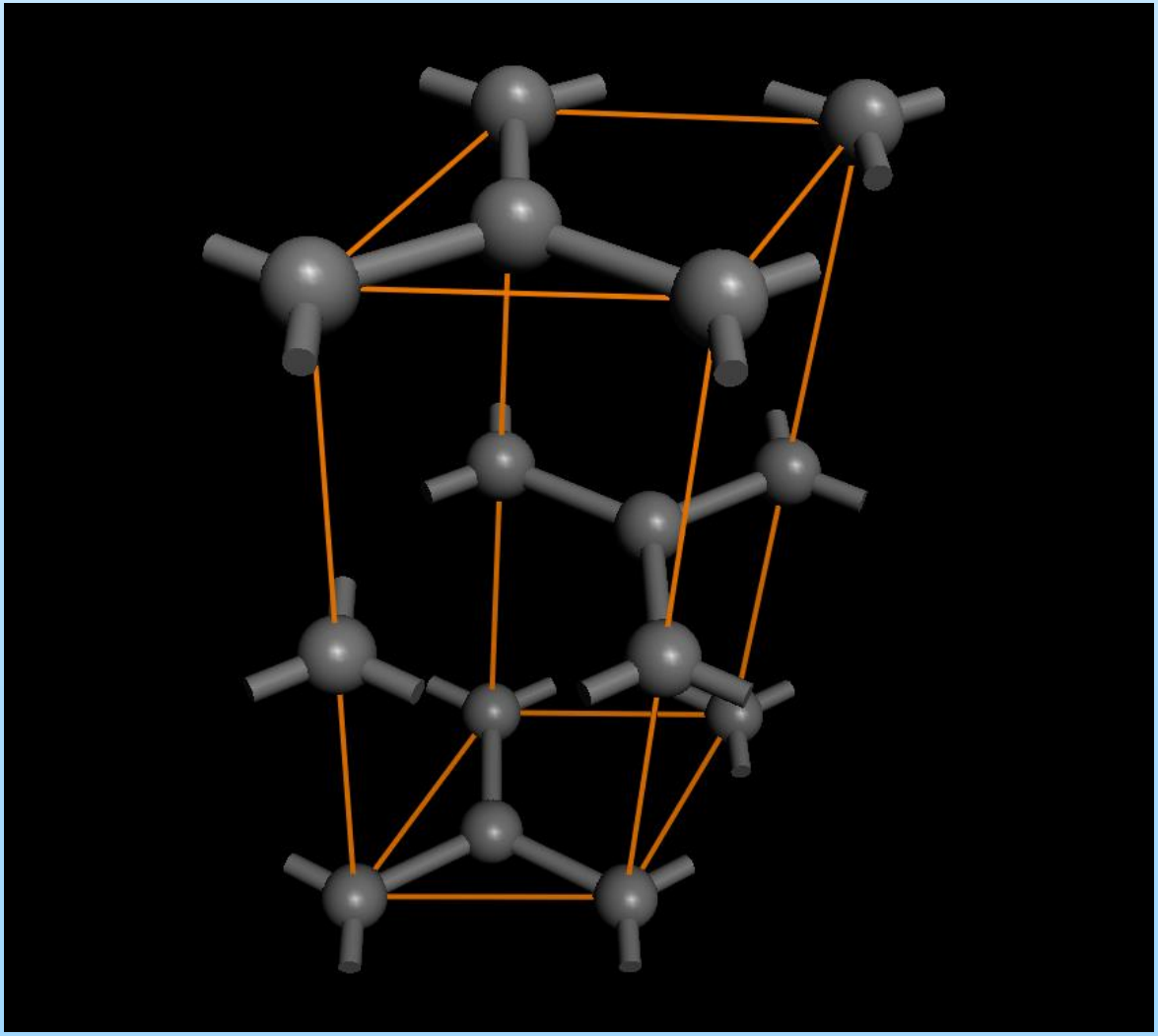

Grafite cella unitaria

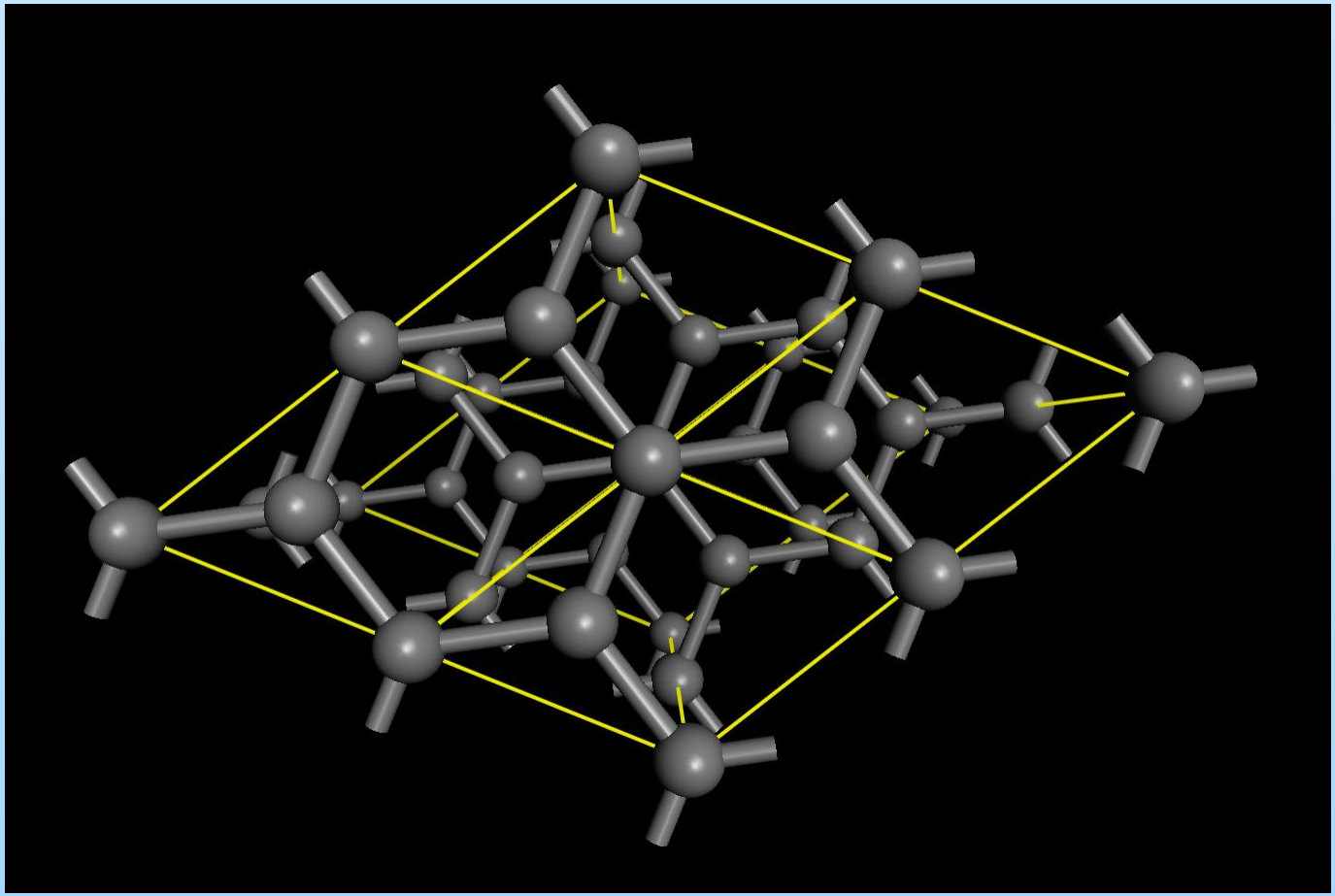

Reticolo reciproco 2D

$$\mathbf{A} = 2\pi \frac{\mathbf{b}\times\mathbf{c}}{\mathbf{a}\cdot\mathbf{b}\times\mathbf{c}}\,; \qquad \mathbf{B} = 2\pi \frac{\mathbf{c}\times\mathbf{a}}{\mathbf{a}\cdot\mathbf{b}\times\mathbf{c}}\,; \qquad \mathbf{C} = 2\pi \frac{\mathbf{a}\times\mathbf{b}}{\mathbf{a}\cdot\mathbf{b}\times\mathbf{c}}\,.$$

ESEMPIO

Reticolo reciproco in due dimensioni. Un reticolo a due dimensioni (fig. 21) ha i vettori base $\mathbf{a} = 2\hat{\mathbf{x}}$; $\mathbf{b} = \hat{\mathbf{x}} + 2\hat{\mathbf{y}}$. Trovare i vettori base del reticolo reciproco.

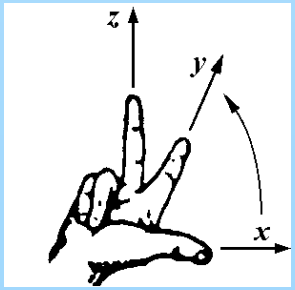

Possiamo usare le nostre definizioni per il caso tridimensionale in questo problema in due dimensioni se supponiamo che **c** sia parallelo all'asse z, per cui il piano dei vettori **A** e **B** del reticolo reciproco sarà nel piano di **a** e **b**. Prendiamo $\mathbf{c} = \hat{\mathbf{z}}$. Ora

$$\mathbf{c}\times\mathbf{a} = \hat{\mathbf{z}}\times(2\hat{\mathbf{x}}) = 2\hat{\mathbf{y}}\,;$$

$$\mathbf{b}\times\mathbf{c} = \hat{\mathbf{x}}\times\hat{\mathbf{z}} + 2\hat{\mathbf{y}}\times\hat{\mathbf{z}} = -\hat{\mathbf{y}} + 2\hat{\mathbf{x}}\,; \qquad \mathbf{a}\cdot\mathbf{b}\times\mathbf{c} = 4.$$

Questi risultati sostituiti nelle (33) danno

$$\mathbf{A} = \pi\hat{\mathbf{x}} - \tfrac{1}{2}\pi\hat{\mathbf{y}}\,; \qquad \mathbf{B} = \pi\hat{\mathbf{y}},$$

come indicato in figura 21.

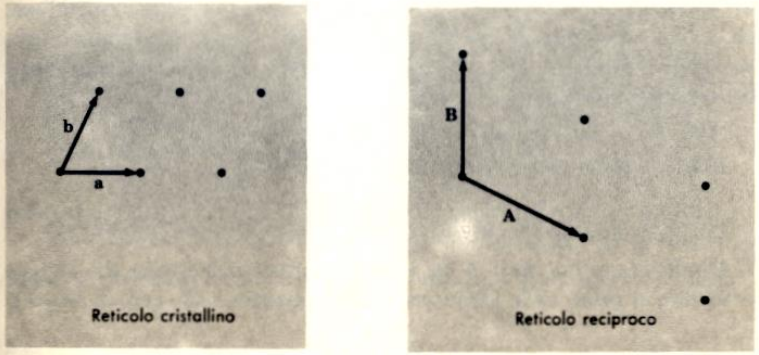

Figura 21 Reticolo reciproco in due dimensioni: **A** e **B** sono perpendicolari a gruppi di piani (linee) nel reticolo cristallino, cioè alle linee parallele rispettivamente a **b** e **a**. Qualsiasi vettore fra punti del reticolo reciproco è perpendicolare a qualche piano nel reticolo cristallino.

Kittel, Introduzione alla fisica dello Stato Solido

Grafene: cella elementare e I zona di Brillouin

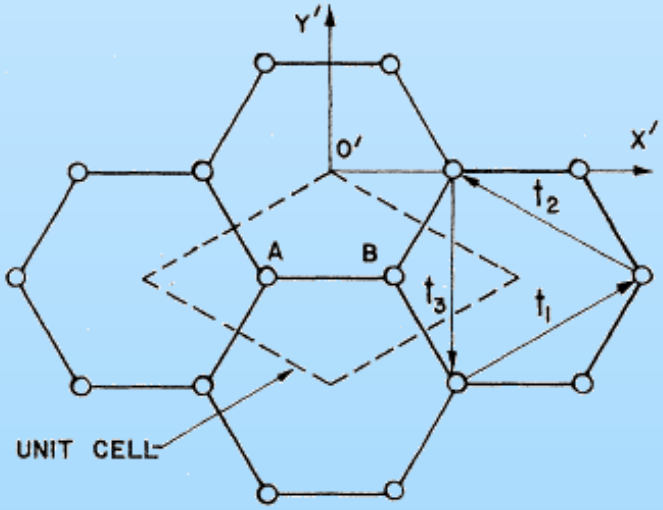

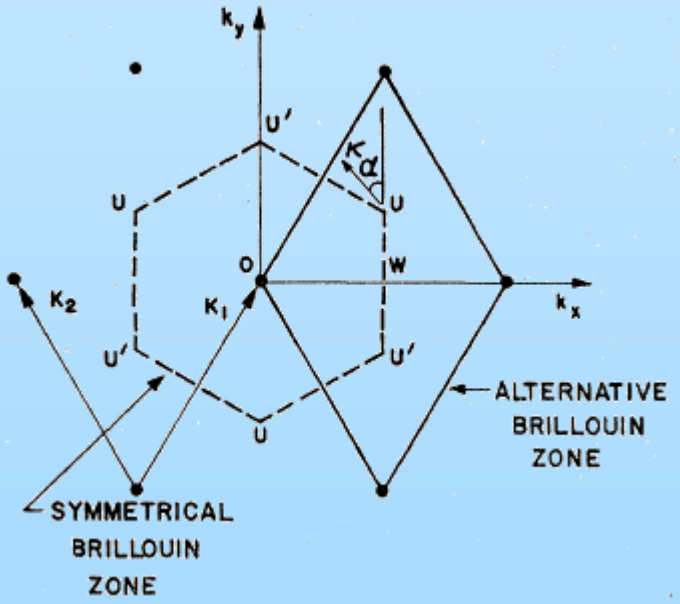

Reticolo reciproco (I zona di B.)

Grafene: cella elementare e I zona di Brillouin

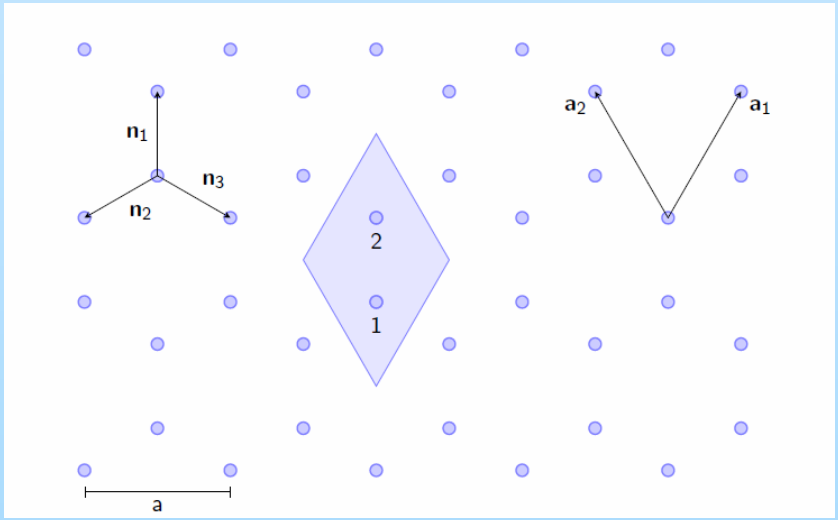

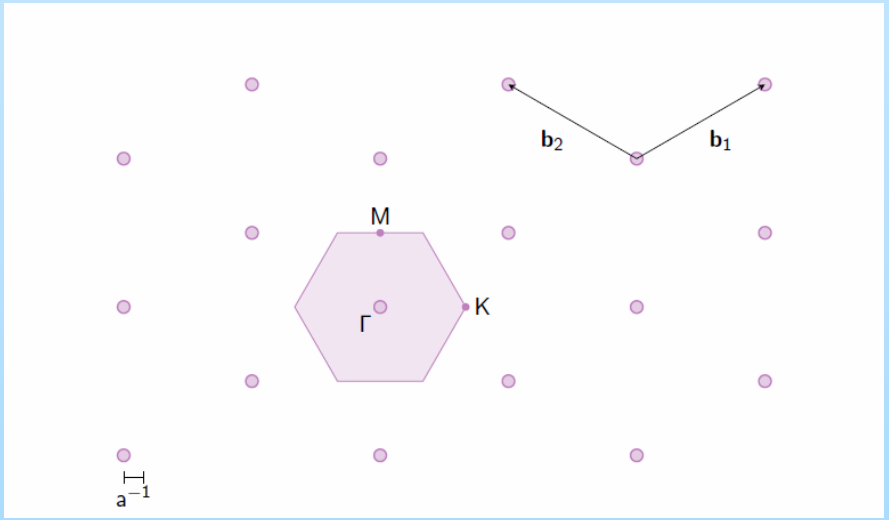

Reticolo diretto: a_1 e a_2 vettori primitivi, n_1, n_2 e n_3 vettori primi vicini

Reticolo reciproco: b_1 e b_2 vettori primitivi, in rosa I zona di B.

Tight Binding (LCAO)

$$\psi(\mathbf{r}) = \sum_{\mathbf{R}} e^{i\mathbf{k}\cdot\mathbf{R}}\phi(\mathbf{r}-\mathbf{R}),$$

ϕ funzioni di Wannier

$$\phi(\mathbf{r}) = \sum_{n} b_n\psi_n(\mathbf{r}).$$

ψ_n orbitali atomici (indicati con X(r) di seguito)

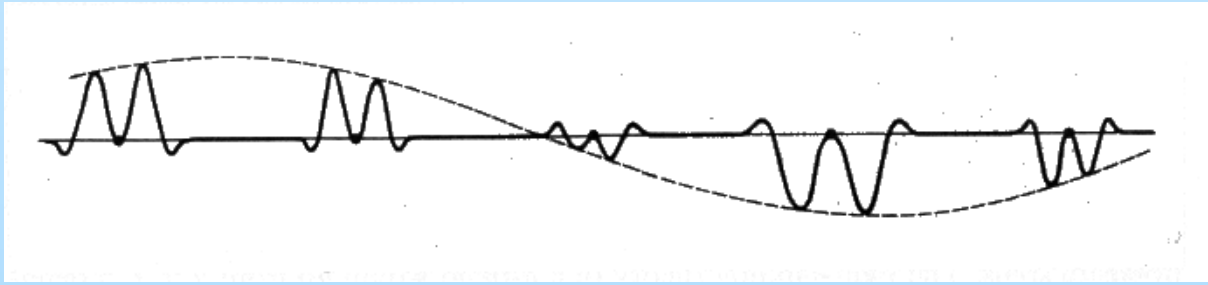

$$\psi(\mathbf{r}+\mathbf{R}) = e^{i\mathbf{k}\cdot\mathbf{R}}\psi(\mathbf{r}).$$

Condizione di Bloch

Se c'è una base nella cella……

$$\psi_{\mathbf{k}}(\mathbf{r}) = \sum_{j\alpha} c_{j\alpha}\, e^{i\mathbf{k}\mathbf{d}_j} \sum_{\mathbf{R}} e^{i\mathbf{k}\mathbf{R}}\, \phi_{j\alpha}(\mathbf{r}-\mathbf{R}-\mathbf{d}_j),$$

dove i $\phi_{j\alpha}(\mathbf{r})$ sono gli orbitali di un singolo atomo isolato di numero atomico Z_j centrato nell'origine, individuati dall'indice $\alpha \in \{1s, 2s, 2p_x \ldots\}$. $\mathbf{R}$ indica un generico vettore del reticolo di Bravais, j è un indice che individua i siti della base del cristallo, $\mathbf{d}_j$ è la posizione del sito j all'interno della cella unitaria ed infine i $c_{j\alpha}$ sono i coefficienti incogniti della combinazione lineare.

Grafene: Proprietà elettroniche

$$\psi_{2\pi} = \frac{1}{\sqrt{3}}[\psi(2S) + \sqrt{2}\psi(2P_x)]$$

$$\psi_{2\pi/3} = \frac{1}{\sqrt{3}}\left[\psi(2S) - \frac{1}{\sqrt{2}}\psi(2P_x) + \sqrt{(3/2)}\psi(2P_y)\right]$$

$$\psi_{4\pi/3} = \frac{1}{\sqrt{3}}\left[\psi(2S) - \frac{1}{\sqrt{2}}\psi(2P_x) - \sqrt{(3/2)}\psi(2P_y)\right]$$

Nel piano

P_z fuori dal piano

$$P_z = \frac{1}{2\sqrt{6a^5}} re^{-\frac{r}{2a}} \sqrt{\frac{3}{8\pi}} \cos\theta$$

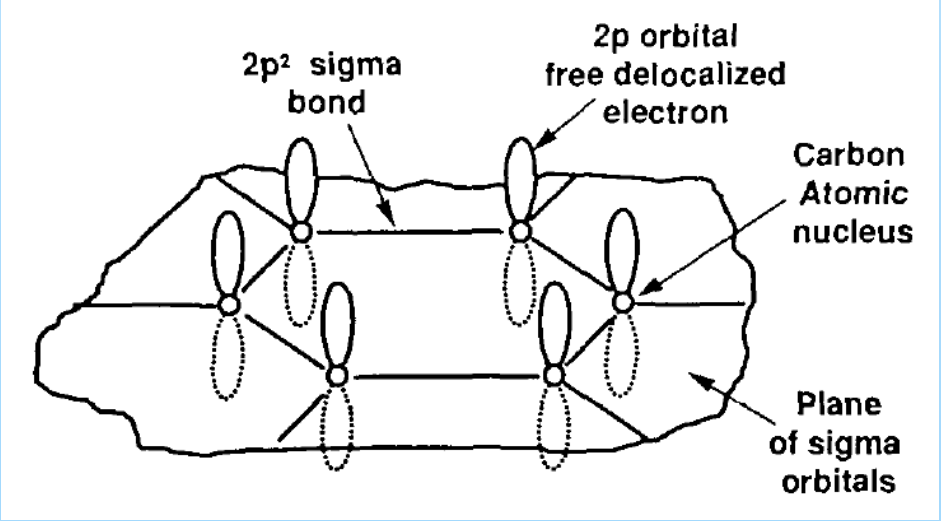

X-ray absorption measurements of high resolving power for potassium, which is expected to show wider departure from free electrons, have been carried out by Platt.[16] The K edge investigated shows quite close agreement with his theoretically predicted absorption which was based on the assumption that the electrons are free. No evidence existed to show an energy gap. This, of course, is at best supporting evidence of the non-existence of a gap in potassium since gaps may exist which could be completely masked by the eigenvalue dependence upon wave vector direction.

[16] J. B. Platt, Phys. Rev. 69, 337 (1946).

ACKNOWLEDGMENTS

The authors are indebted to Dr. W. A. Bowers for permission to publish his results on the five additional states shown in Table IV and also wish to thank Dr. Bowers for continuing the application of the method when the war interrupted the work.

PHYSICAL REVIEW VOLUME 71, NUMBER 9 MAY 1, 1947

The Band Theory of Graphite

P. R. WALLACE*
National Research Council of Canada, Chalk River Laboratory, Chalk River, Ontario
(Received December 19, 1946)

The structure of the electronic energy bands and Brillouin zones for graphite is developed using the "tight binding" approximation. Graphite is found to be a semi-conductor with zero activation energy, i.e., there are no free electrons at zero temperature, but they are created at higher temperatures by excitation to a band contiguous to the highest one which is normally filled. The electrical conductivity is treated with assumptions about the mean free path. It is found to be about 100 times as great parallel to as across crystal planes. A large and anisotropic diamagnetic susceptibility is predicted for the conduction electrons; this is greatest for fields across the layers. The volume optical absorption is accounted for.

1. INTRODUCTION

THE purpose of this paper is to develop a basis for the explanation of some of the physical properties of graphite through the band theory of solids. We shall be concerned primarily with a discussion of its electrical conductivity, but the treatment given makes possible the explanation not only of the electrical conductivity and its anisotropy but also the thermal conductivity, diamagnetic susceptibility, and optical absorption.

The electrical resistivity of single crystals of graphite is about 4 to 6×10^{-5} ohm-cm.[1] This corresponds to a conductivity of the order of that of a poor metal. The temperature coefficient of the conductivity is negative, as in the case of a metal. Polycrystalline graphite, on the other hand, has a much higher resistivity which varies very strongly according to the type of graphite used, and has a *positive* temperature coefficient of conductivity[2] to about 1400°C, and negative thereafter. Since the crystals of commercial graphites tend to be of the order of 10^{-6} cm, and it is quite porous (density $\sim$1.6 as against 2.25 for single crystals), it seems reasonable to attribute the high resistivity of polycrystalline graphite to the crystal boundaries, on which may be lodged impurity atoms. The latter would tend to be driven off on heating, thus accounting for the observed temperature dependence. We shall show, however, that the band theory would seem to make possible the explanation of the conductivity properties of single crystals.

* Now at McGill University.

[1] Given by E. Ryschewitsch, Zeits. f. Elektrochem. ang. physik. Chemie 29, 474 (1923), as $3.9\text{–}6\times10^{-3}$ ohm-cm.

[2] C. A. Hansen, Trans. Am. Electrochem. Soc. 16, 329 (1909) gives 137.5×10^{-3} at 0°C 82.5×10^{-3} at 1400°C.

Tight Binding nel grafene

(Wallace 1946)

Phys. Rev. **71** (1947) 622

$$\psi = \varphi_1 + \lambda\varphi_2$$

$$\left.\begin{aligned}\varphi_1 &= \sum_A \exp[2\pi i\mathbf{k}\cdot\mathbf{r}_A]X(\mathbf{r}-\mathbf{r}_A)\\ \varphi_2 &= \sum_B \exp[2\pi i\mathbf{k}\cdot\mathbf{r}_B]X(\mathbf{r}-\mathbf{r}_B)\end{aligned}\right\}$$

$$\int X(\mathbf{r}-\mathbf{r}_A)X(\mathbf{r}-\mathbf{r}_B)d\tau = 0.$$

Nessuna sovrapposizione tra gli orbitali p^z

$$H\psi = E\psi$$

$$H_{11}+\lambda H_{12} = ES,$$

$$H_{21}+\lambda H_{22} = \lambda ES,$$

$$\begin{vmatrix} H_{11}-ES & H_{12} \\ H_{21} & H_{22}-ES \end{vmatrix} = 0$$

$$H_{11} = \int \phi_1^* H\phi_1 d\tau, \quad H_{12} = H_{21}^* = \int \phi_1^* H\phi_2 d\tau,$$

$$E = \frac{1}{2S}\{H_{11}+H_{22} \pm ((H_{11}-H_{22})^2+4|H_{12}|^2)^{\frac{1}{2}}\}$$

$$H_{22} = \int \phi_2^* H\phi_2 d\tau$$

$$S = \int \phi_1^*\phi_1 d\tau = \int \phi_2^*\phi_2 d\tau. \quad = \text{N (celle nel cr.)}$$

Grafene: Proprietà elettroniche

$H_{11} = H_{22}$ per simmetria

$$H_{11}' = H_{22}' = \frac{1}{N} H_{11} = \frac{1}{N} H_{22},$$

$$H_{12}' = \frac{1}{N} H_{12}$$

$$E = H_{11}' \pm |H_{12}'|.$$

+ fuori, - dentro la zona di B. esagonale

$$\Delta E = 2\,|H_{12}'|$$

$$H_{11}' = \frac{1}{N} \sum_{A,\,A'} \exp[-2\pi i \mathbf{k}\cdot(\mathbf{r}_A - \mathbf{r}_{A'})] \times \int X^*(\mathbf{r}-\mathbf{r}_A) H X(\mathbf{r}-\mathbf{r}_{A'})\, d\tau.$$

ponendo

$$E_0 = \int X^*(\mathbf{r}) H X(\mathbf{r})\, d\tau,$$

$$\gamma_0' = -\int X^*(\mathbf{r}-\boldsymbol{\varrho}') H X(\mathbf{r})\, d\tau,$$

$\boldsymbol{\varrho}' = \mathbf{a}_1$ Vettore che congiunge primi vicini A

$$H_{11}' = E_0 - 2\gamma_0'(\cos 2\pi k_y a + 2\cos \pi k_x a\sqrt{3}\cos \pi k_y a)$$

Grafene: Proprietà elettroniche

$$H = H_0 + (H - H_0)$$

H_0 Hamiltoniana di un atomo di C isolato

$$H - H_0 = V - U < 0$$

V Potenziale periodico del reticolo

U Potenziale di un atomo di C

$$H_0 X = E_0 X$$

$$E_0 = \bar{E} - \int X^*(\mathbf{r})(U - V)X(\mathbf{r})d\tau$$

$$\gamma_0' = \int X^*(\mathbf{r} - \varrho')(U - V)X(\mathbf{r})d\tau > 0$$

$$\gamma_0 = \int X^*(\mathbf{r} - \varrho)(U - V)X(\mathbf{r})d\tau > 0$$

$\varrho = \mathbf{AB}$ Reticoli contigui

$$H_{12}' = -\gamma_0(\exp[-2\pi i k_x(a/\sqrt{3})] + 2\cos\pi k_y a \cdot \exp[2\pi i k_x(a/2\sqrt{3})]),$$

$$|H_{12}|^2 = \gamma_0^2(1 + 4\cos^2\pi k_y a + 4\cos\pi k_y a \cos\pi k_x\sqrt{3}a)$$

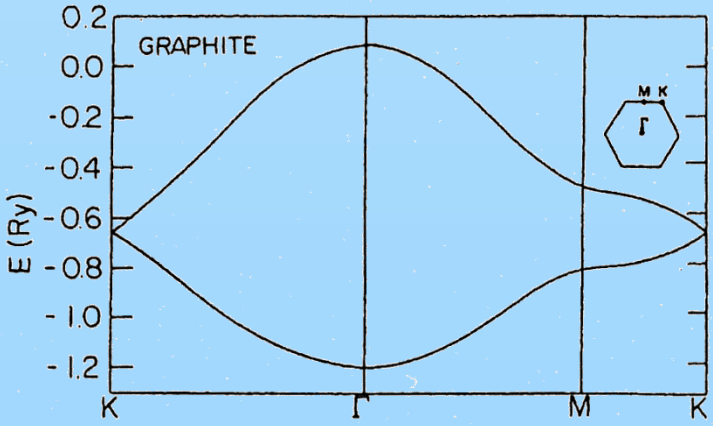

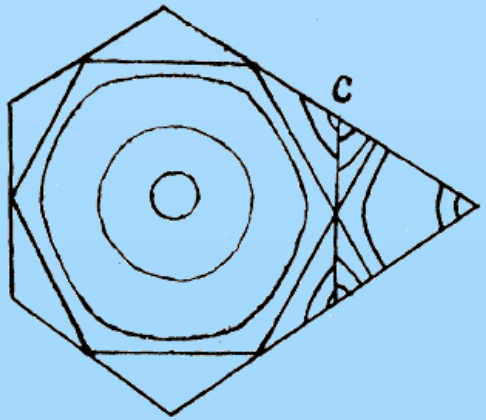

Grafene: Proprietà elettroniche

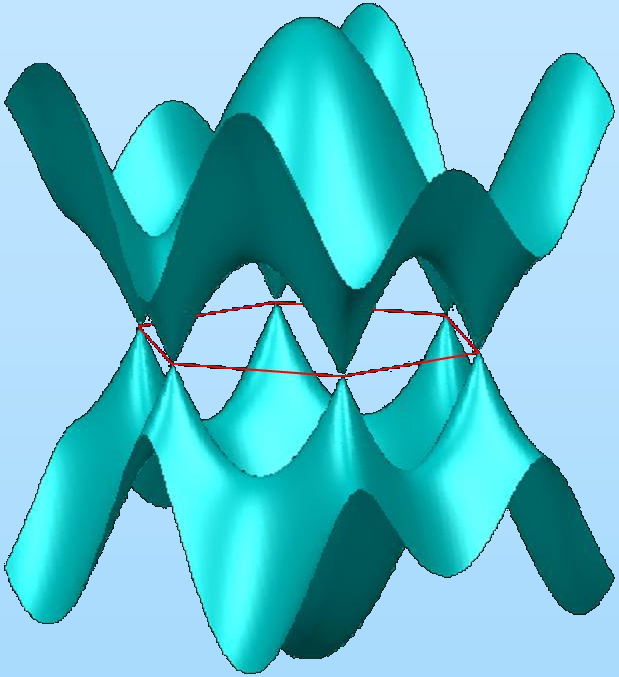

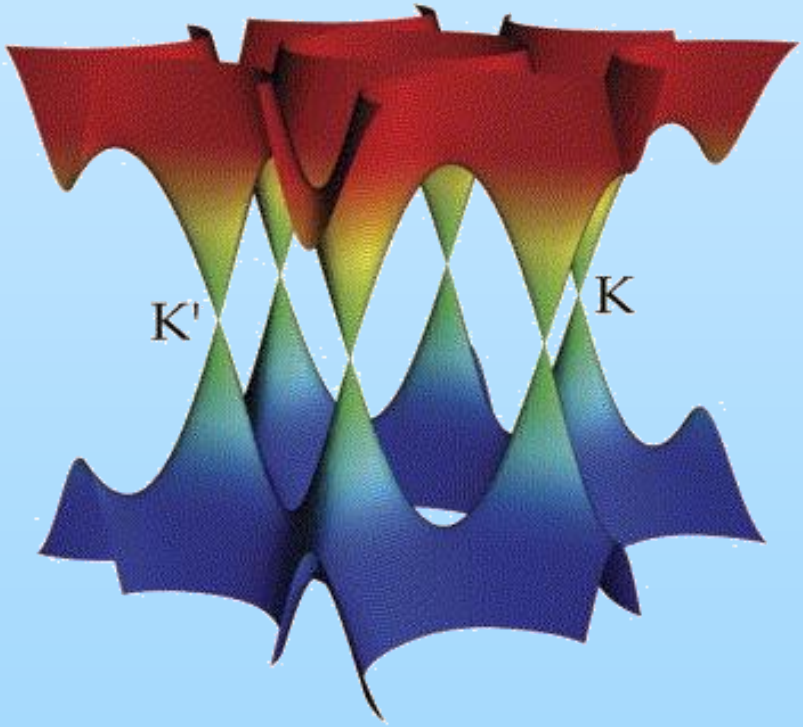

Multigrafene (2 strati)

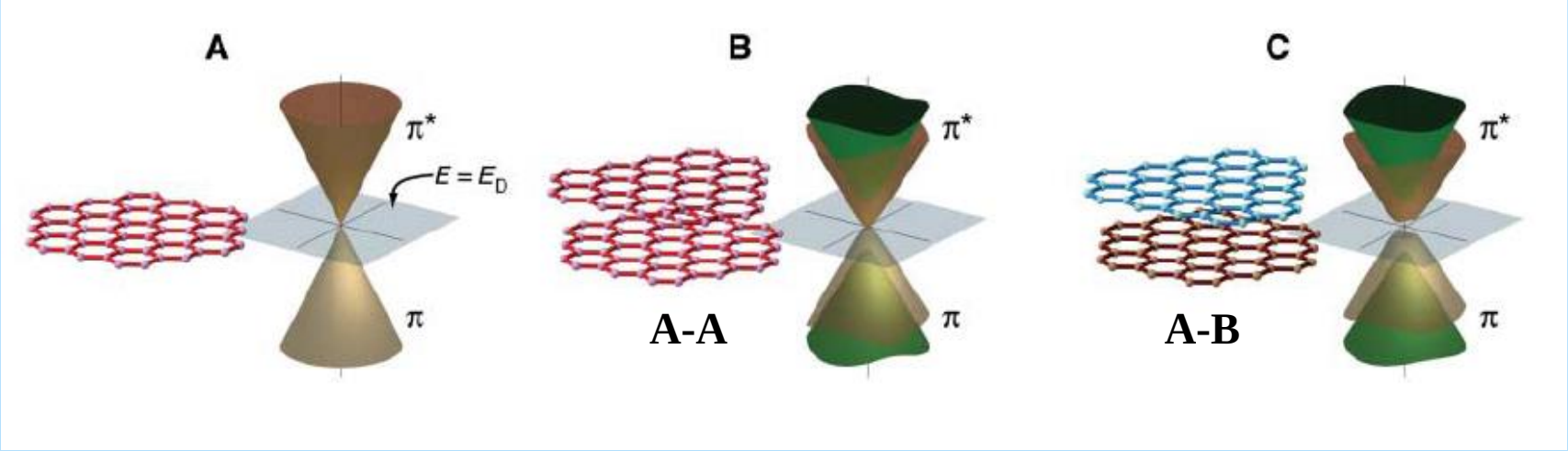

nature materials

ARTICLES

https://doi.org/10.1038/s41563-022-01287-1

Robust superconductivity in magic-angle multilayer graphene family

Jeong Min Park[1,3]✉, Yuan Cao[1,3], Li-Qiao Xia[1], Shuwen Sun[1], Kenji Watanabe[2], Takashi Taniguchi[2] and Pablo Jarillo-Herrero[1]✉

The discovery of correlated states and superconductivity in magic-angle twisted bilayer graphene (MATBG) established a new platform to explore interaction-driven and topological phenomena. However, despite multitudes of correlated phases observed in moiré systems, robust superconductivity appears the least common, found only in MATBG and more recently in magic-angle twisted trilayer graphene. Here we report the experimental realization of superconducting magic-angle twisted four-layer and five-layer graphene, hence establishing alternating twist magic-angle multilayer graphene as a robust family of moiré superconductors. This finding suggests that the flat bands shared by the members play a central role in the superconductivity. Our measurements in parallel magnetic fields, in particular the investigation of Pauli limit violation and spontaneous rotational symmetry breaking, reveal a clear distinction between the $N=2$ and $N>2$-layer structures, consistent with the difference between their orbital responses to magnetic fields. Our results expand the emergent family of moiré superconductors, providing new insight with potential implications for design of new superconducting materials platforms.

Moiré quantum matter results from stacking two or more atomically thin materials with a lattice mismatch or at a relative twist angle[1]. Motivated by the discovery of magic-angle twisted bilayer graphene (MATBG)[2,3], in the past few years moiré systems with different types of constituent layers and structures have been created, hosting a number of correlated and topological states. Phenomena including but not limited to correlated insulators, quantum anomalous Hall effect, ferromagnetism, and generalized Wigner crystals have been discovered and reproduced in various new moiré systems[4–19]. However, for the first few years robust and reproducible moiré superconductivity was seen only in MATBG[3,20,21], despite reports of signatures of superconductivity in a few other systems[5,6,8,9,11,15,22,23].

studied, providing insights into the nature of the correlated states, non-trivial topology and superconductivity[2,3,20,21,30–36]. It has been theoretically shown[37] that for three or more twisted layers of graphene, there are similar series of 'magic' angles if the layers are alternatively twisted by $(\theta,-\theta,\theta,\ldots)$ (Fig. 1a). The values of such angles can be analytically computed from the bilayer value in the chiral limit, where the interlayer hopping at AA sites is turned off[37]. As illustrated in Fig. 1b, they are in fact elegantly related by simple trigonometric transformations, that is the largest magic angle can be expressed as $\theta_N = \theta_\infty \cos\frac{\pi}{N+1}$, where N is the number of layers and $\theta_\infty = 2\theta_{N=2}$ is the asymptotic limit of the largest magic angle as $N\to\infty$. As N increases, the magic angle increases and the moiré length scale decreases. The real magic-angle values deviate slightly

Grafite: Proprietà elettroniche

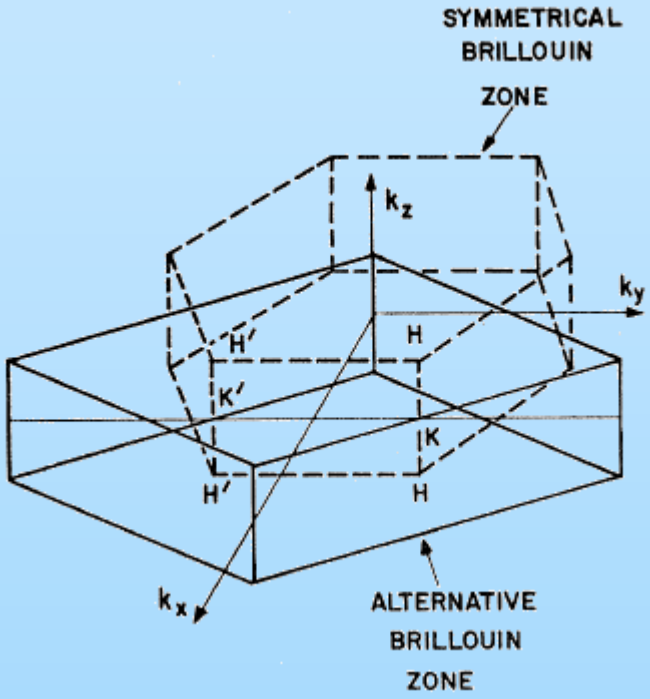

$\gamma_0 >> \gamma_n$

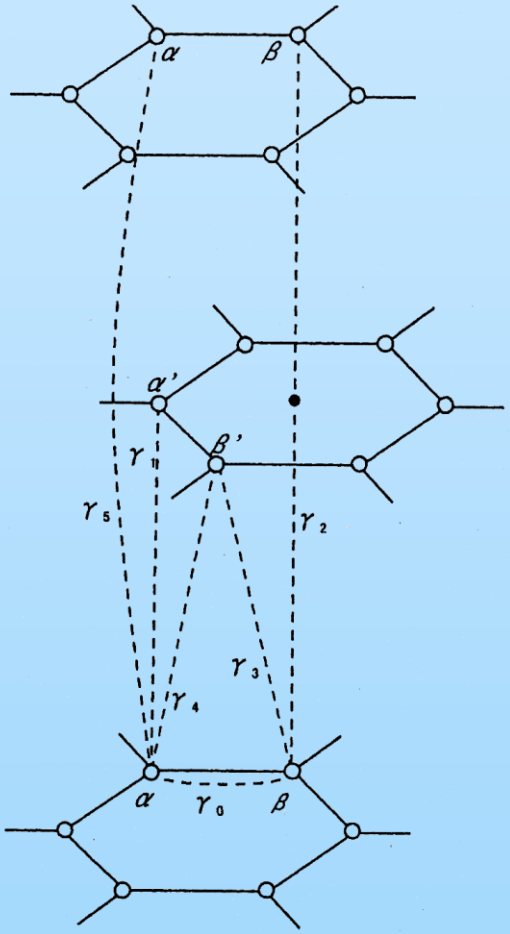

$\gamma_0 = 3.16$, $\gamma_1 = 0.39$,
$\gamma_2 = -0.020$, $\gamma_3 = 0.315$, $\gamma_4 \simeq 0.044$,
$\gamma_5 = 0.038$; $\Delta = -0.008$ eV

Grafite: Proprietà elettroniche

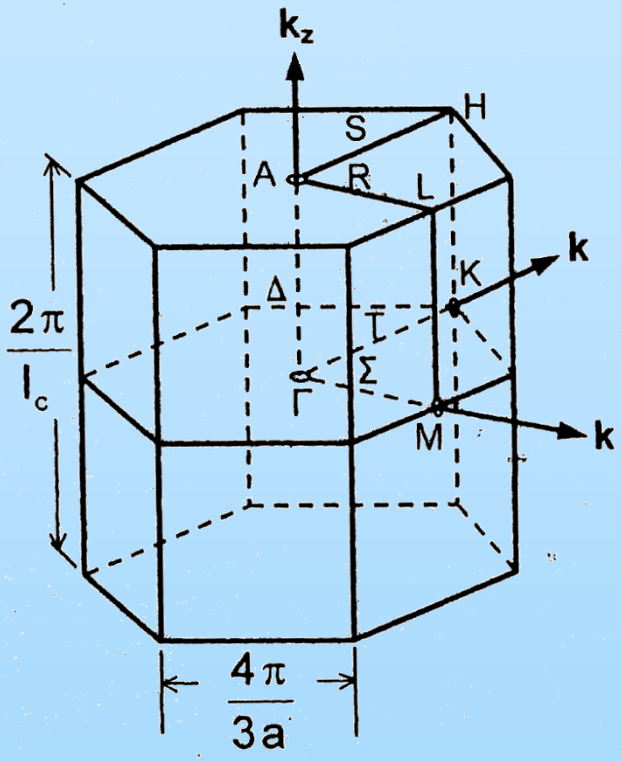

$\gamma_0 = 3.16,\ \gamma_1 = 0.39,$
$\gamma_2 = -0.020,\ \gamma_3 = 0.315,\ \gamma_4 \simeq 0.044,$
$\gamma_5 = 0.038;\ \Delta = -0.008$ eV

4 bande (tratteggiate)

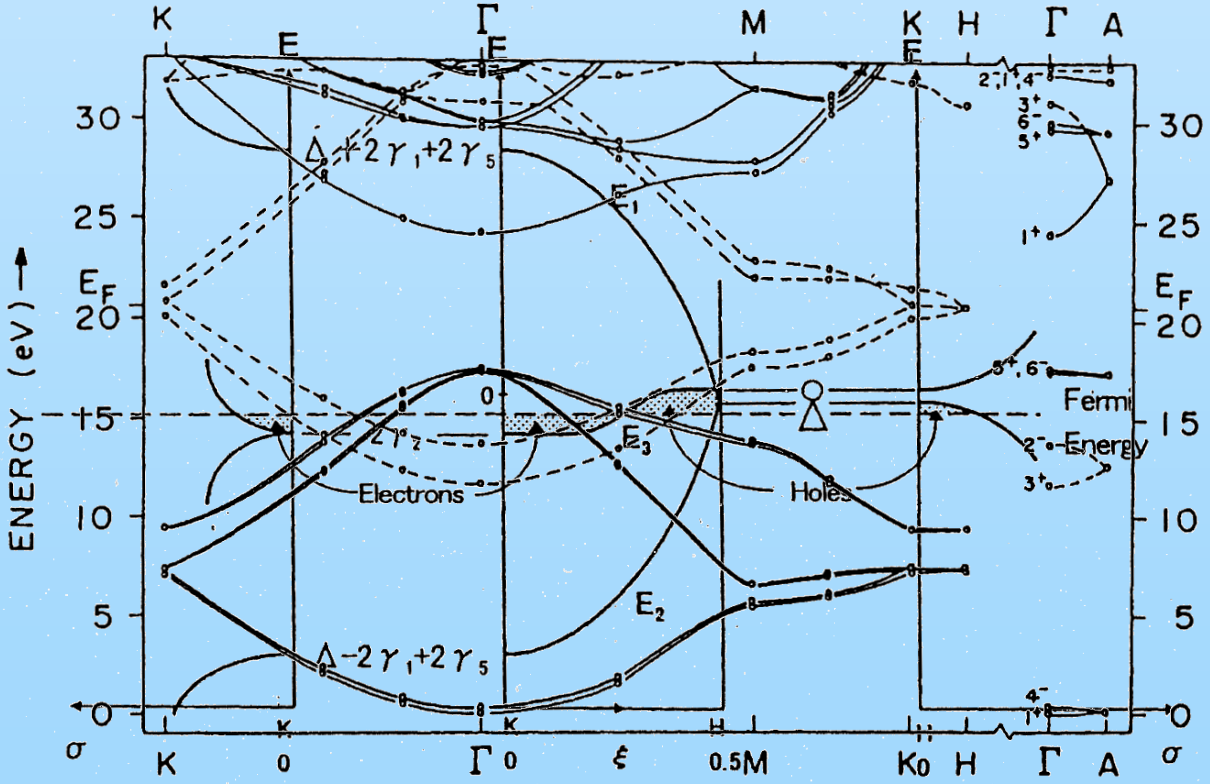

Grafite: Superficie di Fermi

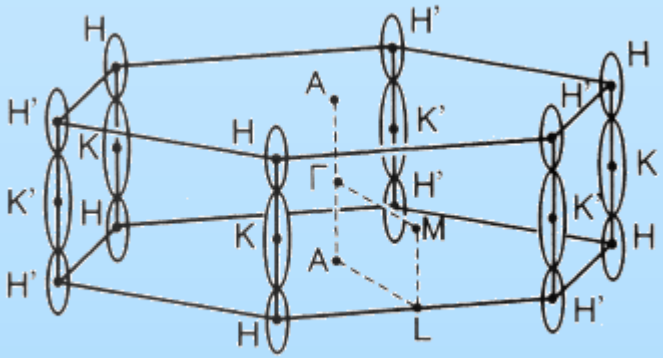

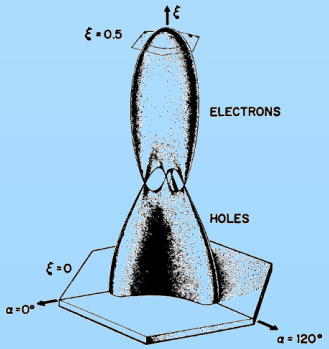

Dresselhaus 1964

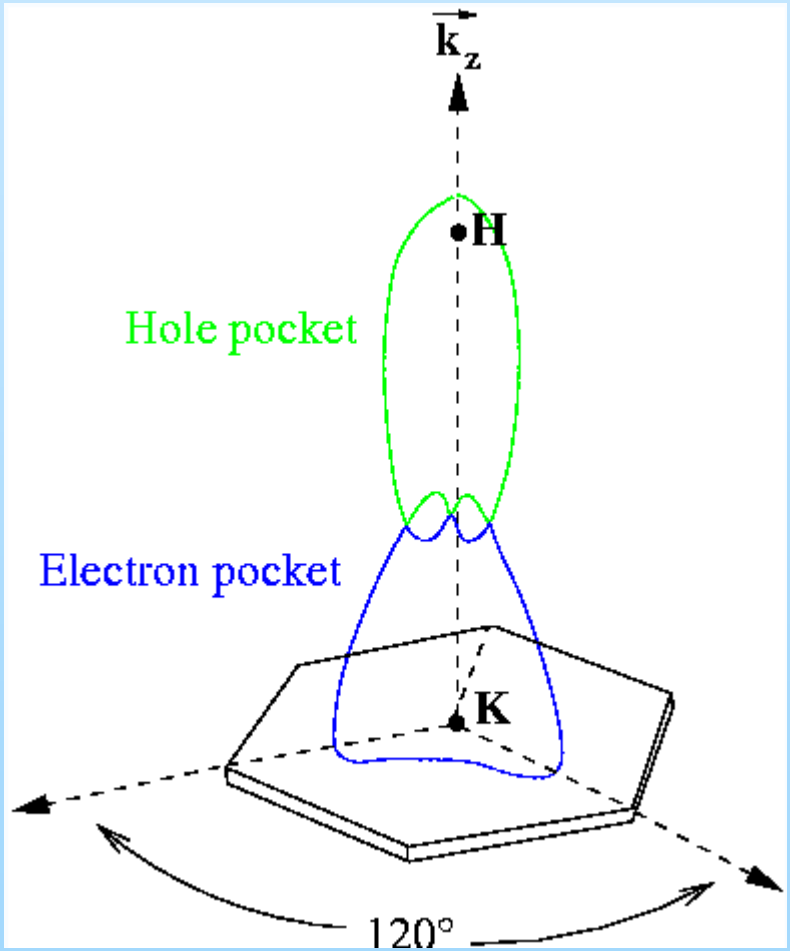

Grafite: Superficie di Fermi

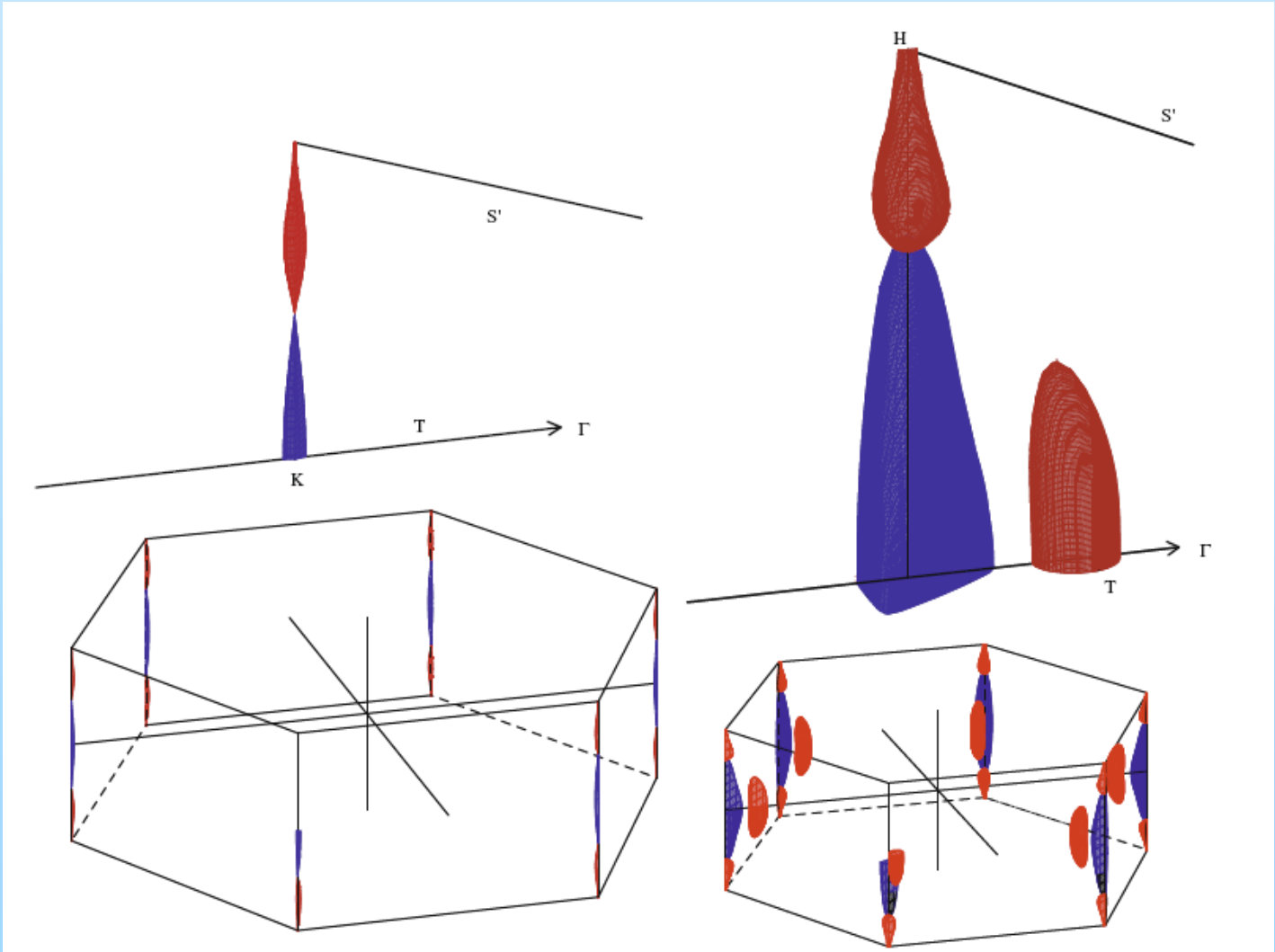

Fig. 4. Fermi surface p=0 (left) and 50 GPa (right).